THE PLANT CELL

CONSTITUTIVE EXPRESSER OF PATHOGENESIS-RELATED GENES 5 is an RNA-binding protein controlling plant immunity via an RNA processing complex

Shun Peng [1,†] Dongbei Guo [1,†] Yuan Guo [1,†] Heyu Zhao [1] Jun Mei [1] Yakun Han [1]
Rui Guan [1] Tianhua Wang [1] Teng Song [1] Keke Sun [1] Yunhan Liu [1] Ting Mao [1]
Huan Chang [1] Jingshi Xue [1] Yingfan Cai [2] Dong Chen [3] and Shui Wang [1,*,‡]

1   College of Life Sciences, Shanghai Normal University, Shanghai 200234, China
2   State Key Laboratory of Cotton Biology, Henan Key Laboratory of Plant Stress Biology, School of Life Sciences, Henan University, Kaifeng, Henan 475001, China
3   Wuhan Ruixing Biotechnology Co., Ltd, Hubei, Wuhan 430075, China

*Author for correspondence: shuiwang@shnu.edu.cn
†Co-first authors
‡Senior author
S.W. and S.P. designed the research. S.P., D.G., Y.G., H.Z., J.M., Y.H., R.G., T.W., T.S., K.S., Y.L., T.M., H.C., J.X., Y.C., D.C., and S.W. performed the experiments. S.W., S.P., D.G., and D.C. analyzed the results. S.W., S.P., and D.G. wrote the article.
The author responsible for distribution of materials integral to the findings presented in this article in accordance with the policy described in the Instructions for Authors (https://academic.oup.com/plcell) is: Shui Wang (shuiwang@shnu.edu.cn)

Abstract

Plant innate immunity is capable of combating diverse and ever evolving pathogens. The plasticity of innate immunity could be boosted by RNA processing. *Arabidopsis thaliana* CONSTITUTIVE EXPRESSER OF PATHOGENESIS-RELATED GENES 5 (CPR5), a key negative immune regulator, is a component of the nuclear pore complex. Here we further identified CPR5 as a component of RNA processing complexes. Through genetic screening, we found that RNA splicing activator NineTeen Complex and RNA polyadenylation factor CLEAVAGE AND POLYADENYLATION SPECIFICITY FACTOR, coordinately function downstream of CPR5 to activate plant immunity. CPR5 and these two regulators form a complex that is localized in nuclear speckles, an RNA processing organelle. Intriguingly, we found that CPR5 is an RNA-binding protein belonging to the Transformer 2 (Tra2) subfamily of the serine/arginine-rich family. The RNA recognition motif of CPR5 protein binds the Tra2-targeted RNA sequence in vitro and is functionally replaceable by those of Tra2 subfamily proteins. In planta, it binds RNAs of CPR5-regulated alternatively spliced genes (ASGs) identified by RNA-seq. *ARGONAUTE 1* (*AGO1*) is one of the ASGs and, consistent with this, the *ago1* mutant suppresses the *cpr5* phenotype. These findings reveal that CPR5 is an RNA-binding protein linking RNA processing with plant immunity.

Introduction

Plants have two layers of defense, pathogen-associated molecular pattern (PAMP)-triggered immunity (PTI) and effector-triggered immunity (ETI), which are mediated by cell-surface pattern-recognition receptors (PRRs) and intracellular nucleotide-binding/leucine-rich repeat receptors (NLRs), respectively. ETI is an intense immune response that is often associated with programmed cell death (PCD), also

IN A NUTSHELL

Background: Immune receptors recognize invading microorganisms and activate immune responses. There are two types of immune systems, innate immunity and adaptive immunity. In animals, innate immunity is activated by a finite number of the germline gene-encoded receptors, whereas adaptive immunity is induced by an infinite number of somatically recombined gene-encoded receptors from T- and B-cells. In plants, innate immunity is the only immune system, as plants have no counterparts of T- and B-cells. Genome sequencing studies have revealed that the number of genes encoding immune receptors in plants is very limited.

Question: It has long been a mystery how plants make use of the limited immune receptor genes to combat diverse and ever-evolving microorganisms. RNA processing is proposed to be an approach to boost the complexity of these genes. What is the signaling link between RNA processing and plant innate immunity?

Findings: Arabidopsis CONSTITUTIVE EXPRESSER OF PATHOGENESIS-RELATED GENES 5 (CPR5) was previously identified as a key immune regulator. In this study, we further identified CPR5 as a novel RNA-binding protein that forms a complex with the RNA processing regulators NTC and CPSF. Intriguingly, the CPR5–NTC–CPSF complex is localized in the RNA processing organelle termed nuclear speckles. Genome-wide profiling of RNA transcripts in Arabidopsis demonstrated that there are about 500 alternatively spliced genes regulated by CPR5. Usually, alternatively spliced transcripts encode either full-length or truncated proteins. The ratio of full-length/truncated immune regulators may determine the specificity and intensity of plant immunity against diverse microorganisms. Therefore, these findings reveal that a novel signaling pathway links RNA processing with plant immunity.

Next steps: We want to explore the role of the identified CPR5-regulated alternatively spliced genes in plant immunity. Also, we want to genetically dissect the signalling pathway through which the RNA processing regulators NTC/CPSF function downstream of CPR5 to modulate plant immunity.

known as the hypersensitive response (Jones and Dangl, 2006). To explore the signaling pathway of ETI, we can take advantage of two types of mutants: auto-immune mutants, such as *suppressor of nonexpresser of pathogenesis-related genes 1* (*npr1*), *constitutive 1* (*snc1*), and lesion-mimic mutants, such as *constitutive expresser of pathogenesis-related genes 5* (*cpr5*). Interestingly, genetic studies reveal that both SNC1 and CPR5 modulate plant immunity through nucleocytoplasmic transportation, suggesting that they share a common signaling pathway (Bowling et al., 1997; Zhang et al., 2003; Johnson et al., 2012; Wang et al., 2014; Gu et al., 2016).

Arabidopsis thaliana SNC1 is an NLR protein. An autoimmune mutant of this gene, *snc1*, exhibits dwarf morphology and heightened immunity, which is suppressed by *enhanced disease susceptibility 1* (*eds1*) mutant, indicating that the *snc1*-induced phenotype results from constitutive activation of plant ETI (Zhang et al., 2003). The screening and characterization of *snc1* suppressors, termed *modifier of snc1* (*mos*), have found that downstream of this NLR, plant immunity is activated by two macromolecular protein complexes: the nuclear pore complex (NPC) and the NineTeen Complex (NTC; Zhang and Li, 2005; Palma et al., 2007; Cheng et al., 2009; Monaghan et al., 2009). The NTC is also called the PRE-MRNA PROCESSING FACTOR 19 (Prp19)/ CELL DIVISION CYCLE 5 LIKE (CDC5L) complex in human and MOS4-associated complex (MAC) in Arabidopsis.

Precursor messenger RNAs (pre-mRNAs) are spliced on a large ribonucleoprotein (RNP) complex, the spliceosome, which is activated by the NTC. It consists of eight core components, Prp19, CDC5L, PLEIOTROPIC REGULATOR 1 (PRL1), SPLICEOSOME-ASSOCIATED PROTEIN CWC15 HOMOLOG (AD-002/HSPC148), PRE-MRNA SPLICING FACTOR 27 (SPF27), DASH COMPLEX SUBUNIT 1 (DAM1), BETA-CATENIN-LIKE PROTEIN 1 (CTNNBL1), and HEAT SHOCK COGNATE PROTEIN 73 (HSP73; Chan et al., 2003). Among these components, Prp19/MAC3a/b, CDC5L/MAC1, PRL1/MAC2, and SPF27/MOS4 had been shown to function downstream of SNC1 to activate plant immunity (Palma et al., 2007; Monaghan et al., 2009). Alternative splicing (AS) of pre-mRNAs has long been implicated in plant immunity (Staiger et al., 2013). For example, AS of *NLR* genes such as the tobacco (*Nicotiana tabacum*) *N* gene and the Arabidopsis *RESISTANCE TO PSEUDOMONAS SYRINGAE 4* (*RPS4*) and *SNC1* genes, has been detected during plant immune responses (Dinesh-Kumar and Baker, 2000; Zhang and Gassmann, 2003; Xu et al., 2011). Some pathogen effectors regulate plant immunity by directly binding to splicing regulators. For example, the type III effector HopU1 of *Pseudomonas syringae* encodes a mono-ADP-ribosyltransferase, which is injected into the plant cells to target several host plant RNA-binding proteins such as GRP7 (Fu et al., 2007). The ADP-ribosylation of two arginine residues within the RNA recognition motif (RRM) domain of GRP7 by HopU1 blocks the binding of GRP7 to the

transcripts of cell-surface PRRs, FLAGELLIN-SENSITIVE 2 and EF-TU RECEPTOR, and ultimately results in compromised PTI (Nicaise et al., 2013).

Besides AS, alternative polyadenylation (APA) of pre-mRNAs has also been shown to modulate plant immunity, especially the CPR5 signaling pathway. APA is carried out by a multiprotein complex called the 3'-end processing complex, consisting of poly(A) polymerase (PAPS) and four multi-subunit complexes including CLEAVAGE AND POLYADENYLATION SPECIFICITY FACTOR (CPSF), CLEAVAGE FACTORs Im and IIm (CFIm and CFIIm), and CLEAVAGE STIMULATION FACTOR. The CPSF complex consists of CPSF160, CPSF100, CPSF73, CPSF30, FACTOR INTERACTING WITH POLY(A) POLYMERASE 1 (FIP1), and WD REPEAT-CONTAINING PROTEIN 33 (Elkon et al., 2013). There are four genes encoding PAPS in Arabidopsis. PAPS1 functions as a negative regulator of plant immunity. The elevated immune response in *paps1* mutants is suppressed by *eds1* or *phytoalexin-deficient 4* (*pad4*) and largely overlaps with that in the *cpr5* mutant (Vi et al., 2013). CPSF30 is the core component of the CPSF complex. The *cpsf30* mutants are more susceptible than wild-type (WT) plants to both *P. syringae* pv. *tomato* (*Pst*) and *Pst/AvrRpm1* (*Pst* carrying the effector gene *AvrRpm1*) and suppress the PCD of lesion-mimic mutants such as *cpr5*, *lesion simulating disease 1* and *mitogen-activated protein kinase 4* (Bruggeman et al., 2014).

In response to pathogen infection, mammals generate both innate and adaptive immune responses, whereas plants depend on innate immune responses. How plants expand the plasticity of innate immunity to confront diverse pathogens has long been a mystery, as the number of plant NLRs is quite limited, whereas pathogen effectors are enormously various and rapidly evolving. There have been plenty of examples demonstrating that AS and/or APA of NLR genes contribute to the intensity of immune response and are regulated by pathogen infection (Li et al., 2015). It appears that the NLR family is one of hotspots targeted by RNA splicing regulators as the average transcript number per Arabidopsis NLR family gene (3.38 $\pm$ 0.28, 568 transcripts/168 genes) is significantly more than that of all genes in the Arabidopsis genome (AtRTD2 dataset, 2.40 $\pm$ 0.01, 82,184 transcripts/ 34,211 genes) (P = 4.34E-06; Zhang et al., 2017a, 2017b). Therefore, RNA processing, including AS and APA, could be a strategy for plants to promptly enhance immune plasticity upon pathogen infection. It has been estimated that in Arabidopsis genome, ~61% of multiexon genes exhibit AS and ~75% of protein-coding genes undergo APA (Pan et al., 2008; Sherstnev et al., 2012). Although the majority of genes in a genome undergo AS and/or APA, which greatly expands RNA diversity, the role of RNA processing in plant immunity is still poorly understood.

Immunity should be tightly controlled as its improper activation is highly detrimental to the organism. Arabidopsis CPR5 was first identified as a negative regulator of plant immunity using the immune reporter *PR2:GUS* (the β-glucuronidase gene driven by the promoter of *PATHOGENESIS-*

RELATED PROTEIN 2). The *cpr5* mutant exhibits dwarf, heightened immunity, and PCD (Bowling et al., 1997). CPR5 was later found to be a nucleoporin and a component of the NPC in plants. A conformational change of CPR5 protein caused by activated NLRs promotes the transport of immune signals from cytoplasm to nucleus and releases the core cell-cycle regulators to keep the balance between plant development and immunity. The transcription of immune genes in *cpr5* mutants is intensively and massively upregulated (UP), and the set of UP genes largely overlaps with those UP in plants infected with an avirulent pathogen (74.9% overlap) but not treated with the PAMP elf18 (11.2% overlap), suggesting that CPR5 is mainly involved in plant ETI (Wang et al., 2014; Gu et al., 2016; Wang, 2017). In this study, we further dissected the CPR5 signaling pathway through a genetic screen for *suppressor of cpr5* (*scpr*) mutants. We found that the two RNA processing complexes, pre-mRNA splicing complex NTC and pre-mRNA polyadenylation complex CPSF, coordinately activate plant immunity downstream of CPR5. These findings further demonstrate that CPR5 and the immune receptor SNC1 share a common downstream signaling pathway as both of them also modulate plant immunity through NTC, in addition to NPC. Therefore, this study further explored the underlying mechanism of how CPR5 modulates plant immunity via RNA processing.

Results

CPR5 controls plant immunity via two RNA processing complexes, NTC and CPSF

CPR5 was characterized as a plant-specific nucleoporin that functions as a negative regulator of plant ETI and PCD (Wang et al., 2014; Gu et al., 2016; Wang, 2017). We conducted a genetic screen to further dissect the CPR5 signaling pathway. Previously, we generated mutants in the *cpr5* background using fast neutron bombardment and applied pathogens to screen for suppressors of *cpr5*-induced resistance (Wang et al., 2014). In this study, to improve the efficiency of mutagenesis, the *cpr5* mutant seeds were mutagenized with ethyl methanesulfonate (EMS). We took advantage of the morphological phenotypes of *cpr5* mutants, such as early senescence (especially in cotyledons) and fewer trichomes resulting from PCD to screen for *scpr* (Figure 1A) (Bowling et al., 1997; Wang et al., 2014; Peng et al., 2020). Trypan blue staining and scanning electron microscopy were carried out and confirmed the rescue of PCD and trichome numbers in *cpr5 scpr* double mutants (Figure 1B; Supplemental Figure S1A).

Among the *scpr* mutants, the two top candidates, *scpr44* and *scpr57*, were cloned by a combination of positional cloning and next-generation sequencing (NGS), which identifies single-nucleotide polymorphisms (SNPs). The *scpr* candidates, which were in the *cpr5* background and originated from the Columbia-0 (Col-0) ecotype, were crossed with Landsberg *erecta* ecotype for positional cloning and back to
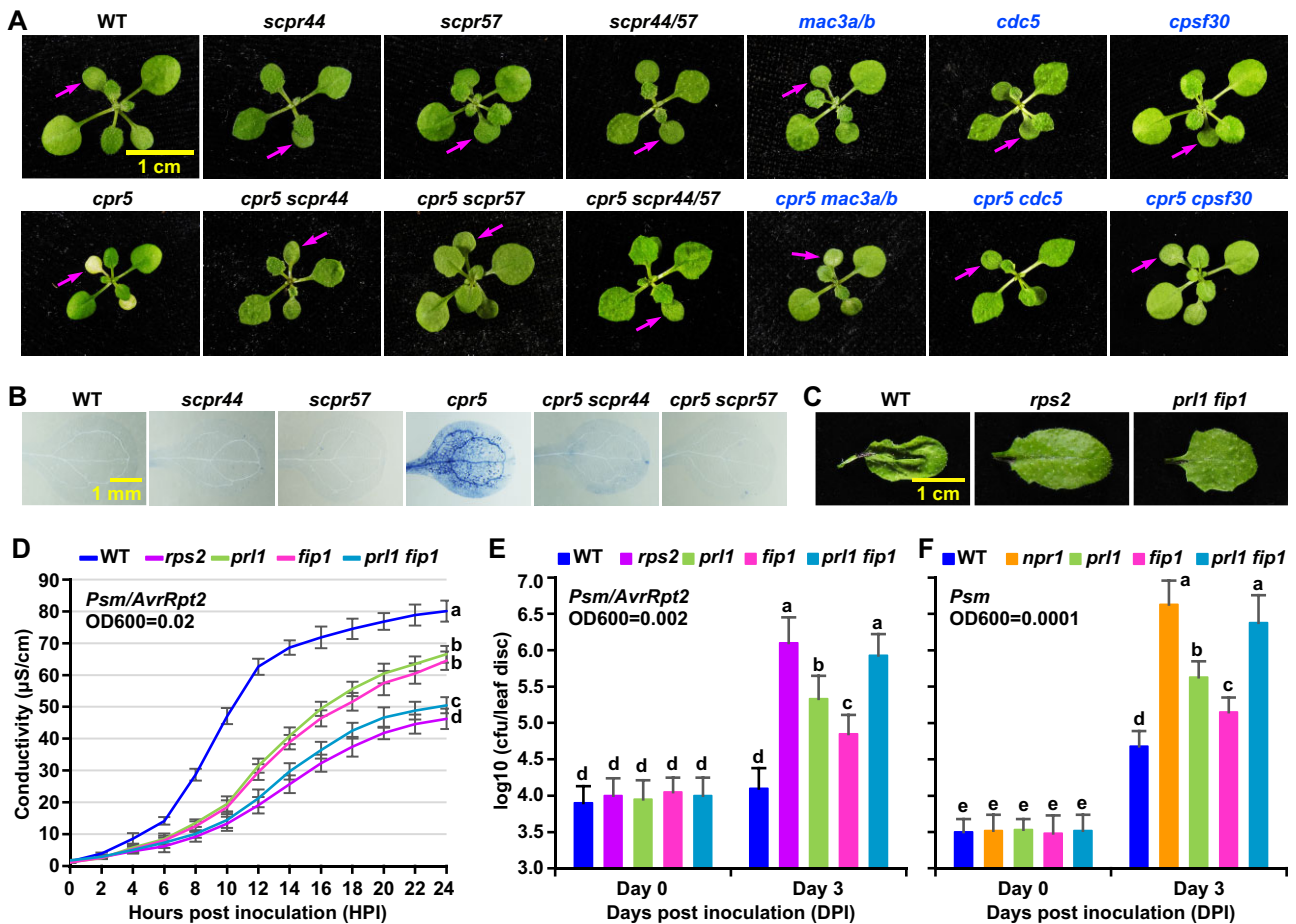
Figure 1 Two RNA processing complexes, NTC and CPSF, coordinately function downstream of CPR5 to activate plant immunity. A, Twelve-day-old WT, *cpr5*, *scpr44*, *cpr5 scpr44*, *scpr57*, *cpr5 scpr57*, *scpr44/57*, *cpr5 scpr44/57*, *mac3a/b*, *cpr5 mac3a/b*, *cdc5*, *cpr5 cdc5*, *cpsf30*, and *cpr5 cpsf30* plants were photographed for early senescence. Cotyledons are indicated (arrows). B, Cotyledons of 12-day-old WT, *cpr5*, *scpr44*, *cpr5 scpr44*, *scpr57*, and *cpr5 scpr57* plants were stained with Trypan blue for cells that had undergone PCD. C, Four-week-old WT, *rps2* and *prl1 fip1* plants were inoculated with *Psm* ES4326 carrying *AvrRpt2* (*Psm/AvrRpt2*) (OD_{600} = 0.02) and photos were taken 10-h postinoculation (HPI). Experiments were conducted 3 times with similar results. D, Four-week-old WT, *rps2*, *prl1*, *fip1*, and *prl1 fip1* plants were inoculated with *Psm/AvrRpt2* (OD_{600} = 0.02). Leaf discs were harvested 50 min after inoculation, and ion leakage was measured every 2 h. Error bars represent standard errors (SES). Experiments were carried out in triplicates. The letter next to the bar at 24 HPI indicates a statistically significant difference between groups at $P < 0.01$. E, Four-week-old WT, *rps2*, *prl1*, *fip1*, and *prl1 fip1* plants were inoculated with *Psm/AvrRpt2* (OD_{600} = 0.002). Bacterial growth (colony-forming unit, cfu) was measured right after inoculation (Day 0) and 3 days later (Day 3). Error bars represent 95% confidence intervals ($n = 8$). Experiments were conducted 3 times with similar results. The letter above the bar indicates a statistically significant difference between groups at $P < 0.01$. F, Four-week-old WT, *npr1*, *prl1*, *fip1*, and *prl1 fip1* plants that were inoculated with *Psm* (OD_{600} = 0.0001). Bacterial growth (cfu) was measured right after inoculation (Day 0) and 3 days later (Day 3). Error bars represent 95% confidence intervals ($n = 8$). Experiments were conducted 3 times with similar results. The letter above the bar indicates a statistically significant difference between groups at $P < 0.01$.

cpr5 mutant to get a pool of about 100 individual *cpr5 scpr* double mutants in an F2 population for NGS.

The results show that the top candidate for *scpr44* is a C to T substitution leading to a nonsense mutation (from CGA coding for R348 to TGA) in the 13th exon of At4g15900 (Supplemental Figure S1B; Supplemental Table S1). At4g15900 encodes the pre-mRNA splicing factor PRL1. The morphological phenotype, such as narrow and serrated leaves, of the *scpr44* mutant fully matches that of the reported *prl1* mutant as well as the T-DNA insertion line SALK_202998 (*prl1-T*) obtained from the Arabidopsis Biological Resource Center (ABRC), suggesting *PRL1* is a strong candidate for *SCPR44* (Nemeth et al., 1998). Like

scpr44, *prl1-T* suppressed the *cpr5* phenotype. Moreover, the *scpr44* mutant was fully complemented by the genomic DNA fragment of the whole *PRL1* gene, further validating that *PRL1* is the *SCPR44* gene (Supplemental Figure S1C).

The top candidate for *scpr57* is a G to A substitution at the 5′-GT donor splice site (altered to AT) of the fourth intron of AT5G58040 (Supplemental Figure S1B; Supplemental Table S1). AT5G58040 encodes the pre-mRNA polyadenylation protein FIP1 (Preker et al., 1995). The morphological phenotype, such as large cotyledons and short hypocotyls, of *scpr57* mutant fully resembles that of a T-DNA insertion line SALK_099558 (*fip1-T*) obtained from ABRC, suggesting that *FIP1* is a strong candidate for *SCPR57*. Like *scpr57*, *fip1-*

T suppressed the *cpr5* phenotype. Moreover, the *scpr57* mutant was complemented by the genomic DNA fragment of the whole *FIP1* gene, further validating that *FIP1* is the *SCPR57* gene (Supplemental Figure S1C).

On the one hand, PRL1 is a core component of the NTC, which is required for remodeling and activating the spliceosome (Wan et al., 2020). Intriguingly, PRL1 and other core components of the NTC, including SPF27/MOS4, PRP19/MAC3 (two copies, MAC3A and MAC3B, in Arabidopsis), and CDC5/MAC1 were found to function downstream of the NLR immune receptor SNC1 to activate plant immunity (Palma et al., 2007; Monaghan et al., 2009). We crossed the *cpr5* mutant with *mac3a/b* and *cdc5* mutants and found that the *cpr5* phenotype was suppressed by these mutants, suggesting that the whole NTC is involved in the CPR5 signaling pathway (Figure 1A). On the other hand, FIP1 is a core component of CPSF (Tian and Manley, 2017). Interestingly, it has been reported that mutation of *CPSF30*, another core component of this complex, also suppressed the *cpr5* phenotype, suggesting that the whole CPSF complex is involved in the CPR5 signaling pathway (Figure 1A) (Bruggeman et al., 2014).

Since both NTC and CPSF are pre-mRNA processing complexes, we further investigated the epistatic interaction between them. The *cpr5*-induced PCD can be suppressed by either *prl1* or *fip1* single mutant, at the early developmental stage, up to 15 days postgermination (DPG) (Figure 1, A and B). However, by 21 DPG, the suppression of *cpr5*-induced PCD by either *prl1* or *fip1* single mutant gradually decreased, whereas that by *prl1 fip1* double mutant remained, suggesting that there is a synergistic epistatic interaction between PRL1 and FIP1 in activating *cpr5*-induced PCD (Supplemental Figure S1D).

Infection with a virulent pathogen *P. syringae pv. maculicola* (Psm) ES4326 and an avirulent pathogen *Psm* carrying the effector gene *AvrRpt2* (Psm/AvrRpt2) validated that the *cpr5*-induced basal immunity and ETI were both suppressed by either *prl1* or *fip1* mutant, indicating that both PRL1 and FIP1 function downstream of CPR5 to activate plant immunity (Supplemental Figure S1, E–G).

To examine the epistatic interaction between PRL1 and FIP1 in plant immunity, we first infected plants with *Psm/AvrRpt2* and found that as compared to the WT plants, the effector-triggered PCD, ion leakage, and immunity were largely compromised in either *prl1* or *fip1* single mutant, whereas those were further compromised in *prl1 fip1* double mutant, almost as much as those in the cognate receptor mutant *rps2*, indicating that there is also a synergistic epistatic interaction between PRL1 and FIP1 in modulating plant effector-triggered PCD and ETI (Figure 1, C–E; Kunkel et al., 1993). We then infected plants with *Psm* and found that as compared to that in WT plants, plant basal immunity was largely compromised in *prl1* or *fip1* single mutants, whereas that in the *prl1 fip1* double mutant was further compromised, almost as much as that in the salicylic acid (SA)-insensitive mutant *npr1*, indicating that there is also a

synergistic epistatic interaction between PRL1 and FIP1 in modulating plant basal immunity (Figure 1F; Cao et al., 1997).

The NTC/CPSF complex is responsible for the *cpr5*-induced immune response

In response to pathogen infection, plant cells reprogram transcription to switch from development to defense (Moore et al., 2011). CPR5 is a negative regulator of plant immunity (Bowling et al., 1997; Wang et al., 2014). RNA-seq analysis revealed that the majority of differentially expressed genes (DEGs) (*cpr5* versus WT, fold change (FC) > 2, $P < 0.05$) in the *cpr5* mutant were UP (2,730/3,751 = 72.78%). There were 1,381 DEGs overlapped between CPR5-regulated DEGs (3,751) and *cpr5 prl1 fip1*-induced DEGs (2,986, *cpr5 prl1 fip1* versus WT, FC > 2, $P < 0.05$), indicating that about two-thirds of CPR5-regulated DEGs (2,370/3,751 = 63.18%) are dependent on PRL1/FIP1 (Figure 2A; Supplemental Figure S2A; Supplemental Data Set 1A). Moreover, principal component analysis showed that the transcriptional profiling of WT, *prl1 fip1*, and *cpr5 prl1 fip1* is significantly different from that of *cpr5* mutants (Supplemental Figure S2B). Gene ontology (GO) enrichment analysis found that plant defense is the top signaling pathway ($P = 1.74E-19$) among the CPR5-regulated and PRL1/FIP1-dependent DEGs (Figure 2B; Supplemental Data Set 1B), such as the defense marker *PATHOGENESIS-RELATED 1* (*PR1*), *PR2*, *AVRRPT2-INDUCED GENE 1* (*AIG1*), *LATE UPREGULATED IN RESPONSE TO HYALOPERONOSPORA PARASITICA 1* (*LURP1*), *DOWNY MILDEW RESISTANT 6* (*DMR6*), the core immune regulators *EDS1* and *PAD4*, the key SA biosynthesis enzymes and regulators *ISOCHORISMATE SYNTHASE 1* (*ICS1*), *AVRPPHB SUSCEPTIBLE 3* (*PBS3*), and *EDS5*, as well as the key systemic acquired resistance (SAR) regulators *AZELAIC ACID INDUCED 1* (*AZI1*), *CALMODULIN BINDING PROTEIN 60-LIKE g* (*CBP60g*), *FLAVIN-DEPENDENT MONOOXYGENASE 1* (*FMO1*), *SAR DEFICIENT 1* (*SARD1*), and *SARD4* (Figure 2C). Reverse transcription-quantitative polymerase chain reaction (RT-qPCR) of plant immune response marker genes *PR1* and *PR2* was performed and validated that the PRL1/FIP1 complex is required for *cpr5*-induced plant immune response (Figure 2D). These data are consistent with the notion that CPR5 is a negative regulator of plant immunity and indicate that PRL1 and FIP1 function downstream of CPR5 to activate immune response (Figures 1 and 2; Wang et al., 2014; Gu et al., 2016).

CPR5 is an RNA-binding protein belonging to an atypical SR subfamily

CPR5 proteins, especially the C-terminal transmembrane (TM) domains, are highly conserved across the plant kingdom from algae, mosses, ferns, and gymnosperms to angiosperms (Supplemental Figure S3A). However, besides the TM domains, we have not identified any other domain of known function in CPR5 proteins through searches in the
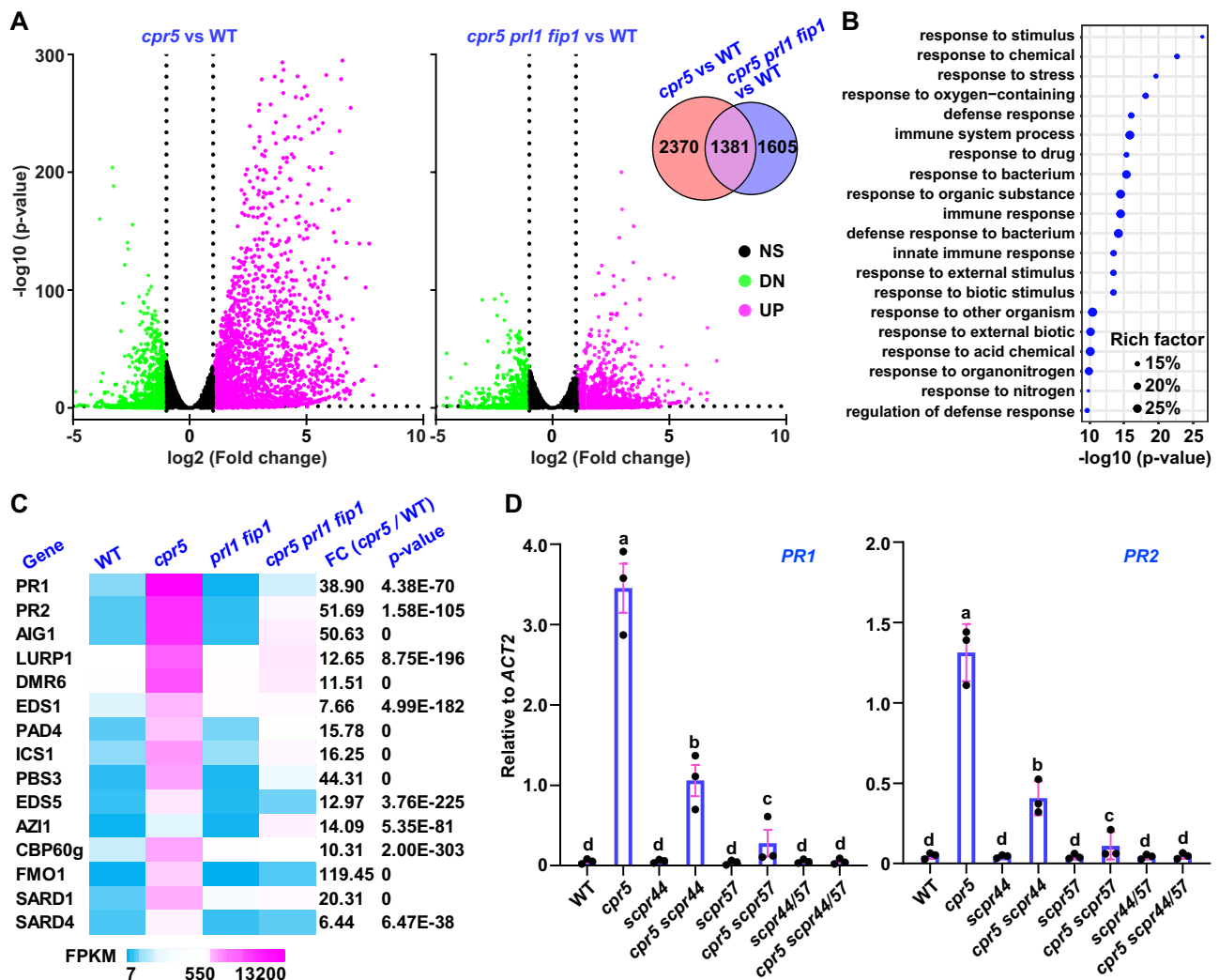
Figure 2 PRL1 and FIP1 mediate *cpr5*-induced immune response. A, Volcano plots illustrating DEGs of *cpr5* versus WT (*cpr5*/WT) and *cpr5 prl1 fip1* vs WT (*cpr5 prl1 fip1*/WT). RNA-seq data are available in the SRA database under the Bioproject accession number PRJNA737003. The *x*-axis represents log2 FC (*cpr5*/WT or *cpr5 prl1 fip1*/WT) and the *y*-axis represents −log10 *P*-value. NS, not significant; UP, up-regulated; DN, down-regulated. Inset: Venn diagram proportionally shows the overlap between 3,751 *cpr5*-altered DEGs (*cpr5*/WT, FC > 2, *P* < 0.05) and 2,986 *cpr5 prl1 fip1*- altered DEGs (*cpr5 prl1 fip1*/WT, FFC > 2, *P* < 0.05). B, GO enrichment analysis of 2,370 DEGs which are altered in *cpr5* mutants (*P* < 0.05, FC > 2) and depend on PRL1/FIP1 (*cpr5 prl1 fip1* versus WT, FC < 2, *P* > 0.05). The bubble chart shows biological process enrichment of DEGs. The *y*-axis represents biological process. The *x*-axis represents the enrichment significance (−log10 *P*-value). Size of the bubble represents rich factor, which is the ratio of the amount of DEGs enriched in a biological process and the amount of all genes annotated in this biological process. C, Heatmap showing RNA-seq data of plant immune marker genes including *PR1/2, AIG1, LURP1, DMR6, EDS1, PAD4, ICS1, PBS3, EDS5, AZI1, CBP60g, FMO1, SARD1, and SARD4*. The FC of *cpr5*/WT as well as its *P*-values are indicated. D, qPCR was carried out on *PR1* (left) and *PR2* (right) in 12-day-old seedlings of WT, *cpr5, scpr44, cpr5 scpr44, scpr57, cpr5 scpr57, scpr44/57,* and *cpr5 scpr44/57. ACT2* was used as an internal control. Error bars represent SEs. Experiments were conducted in triplicate. The letter above the bar indicates a statistically significant difference between groups at *P* < 0.01.

Conserved Domain of National Center for Biotechnology Information (NCBI). We, therefore, aligned the CPR5 proteins from various plant species to identify conserved sequences.

First, we discovered a conserved serine/arginine-rich (SR) domain in the very beginning of the N-terminus, with a motif pattern of [kr](3)-x(5,30)-[st](4)-x(5,30)-[kr](3) (Figure 3A). SR superfamily proteins contain one or two RRM domains and an SR domain. Typically, the SR domain is localized to the C-terminus of RRM domain, here designated as the RRM-SR domain structure. We then searched the SR motif pattern of CPR5 for proteins with SR domain at the N-terminus of RRM domain, designated as the SR-RRM domain structure, and found that human RNA-BINDING PROTEIN WITH SERINE-RICH DOMAIN 1 (RNPS1) is a candidate protein with this structure (Figure 3B; Califice et al., 2012). However, the overall similarity between CPR5 and RNPS1 is very poor. We further looked for plant homologs of RNPS1 and found that plant SERINE/ARGININE-RICH 45 (SR45) and SR45a are the proteins with the highest similarity to RNPS1, especially in the RRM domain (Supplemental Figure S3, B and C). These
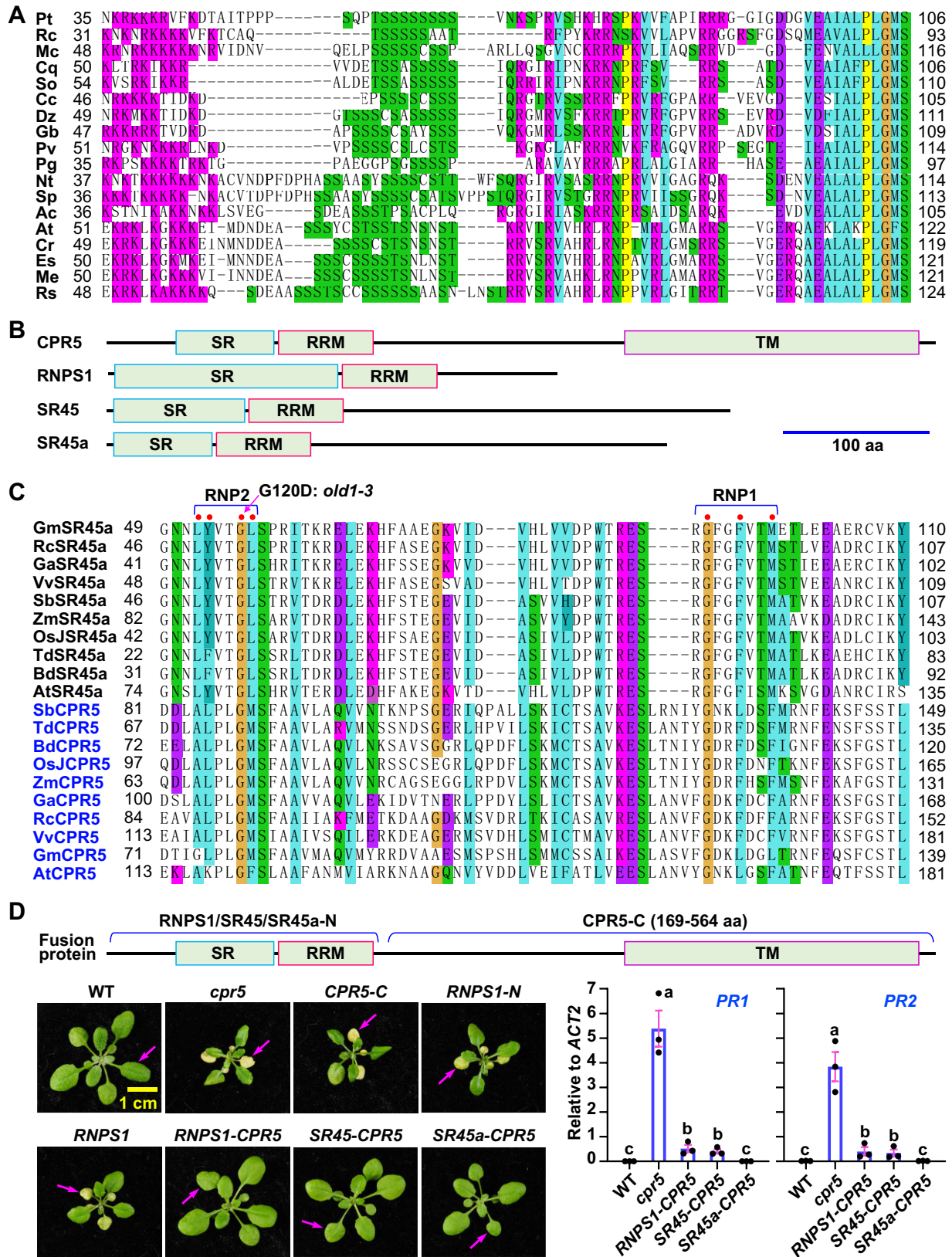
Figure 3 CPR5 is an RNA-binding protein of the SR family. A, The putative SR domain. Alignment of the N-termini of CPR5 proteins using ClustalX2 (http://www.clustal.org/clustal2/). Plant species include *A. thaliana* (*At*), *Actinidia chinensis* (*Ac*), *Capsella rubella* (*Cr*), *Chenopodium quinoa* (*Cq*), *Corchorus capsularis* (*Cc*), *Durio zibethinus* (*Dz*), *Eutrema salsugineum* (*Es*), *Gossypium barbadense* (*Gb*), *Microthlaspi erraticum* (*Me*), *Momordica charantia* (*Mc*), *N. tabacum* (*Nt*), *Pistacia vera* (*Pv*), *Populus trichocarpa* (*Pt*), *Punica granatum* (*Pg*), *Raphanus sativus* (*Rs*), *Ricinus communis* (*Rc*), *Spinacia oleracea* (*So*), and *Solanum pennellii* (*Sp*). B, The protein structures of CPR5, RNPS1 (human), SR45 (AT1G16610) and SR45a

proteins belong to the Transformer-2 (Tra2) subfamily of the SR superfamily (Figure 3B; Hoshijima et al., 1991; Califice et al., 2012). Phylogenetic analysis of Tra2 subfamily proteins from animals and plants revealed that in terms of RRM domains, plant SR45 and SR45a are homologs of human RNPS1 and Tra2, respectively (Supplemental Figure S3, D and E; Supplemental File S1; Tacke et al., 1998).

RRM domain contains two short consensus sequences (R/K)-G-(F/Y)-(G/A)-(F/Y)-V-X-(F/Y) and (L/I)-(F/Y)-(V/I)-X-(N/G)-L, referred to as RNP1 and RNP2, respectively (Califice et al., 2012). Intriguingly, we aligned Tra2, RNPS1, SR45, and SR45a together with CPR5 and found that CPR5 bore an RRM domain which is mostly similar to that of SR45a. Especially, the RNP1 and RNP2 motifs of CPR5 proteins are highly conserved across plant species as well as between CPR5 and SR45a proteins (Figure 3C; Supplemental Figure S3, D and E). The essence of RRM domain to CPR5 protein is indicated in a cpr5 mutant allele, old1-3, which has G120D mutation within the putative RNP2 motif, identified though a genetic screening for early senescence and later found to be critical to CPR5 homomeric interaction (Jing et al., 2007; Gu et al., 2016).

To explore if the SR-RRM domain is essential for CPR5 function, we transferred the C-terminus of CPR5 protein (CPR5-C; 169–564 amino acid [aa]), in which the SR-RRM domain was removed, and the N-terminal SR-RRM domain of human RNPS1 (RNPS1-N; 1–240 aa) into cpr5 mutant. The results showed that both CPR5-C and RNPS1-N cannot complement the cpr5 mutant, suggesting that the SR-RRM domain is essential for CPR5 function, but is not itself sufficient for CPR5 function. We also found that the full-length RNPS1 did not rescue the cpr5 mutant. We then fused RNPS1-N to the N-terminus of CPR5-C to generate FUSE–RNPS1–CPR5 and transferred it into cpr5 mutant. Surprisingly, the RNPS1–N/CPR5-C fusion protein can complement the cpr5 mutant (Figure 3D). Meanwhile, we also fused the N-terminal SR-RRM domain of SR45 (SR45-N; 1–176 aa) or SR45a (SR45a-N; 1–131 aa) to CPR5-C to generate FUSE–SR45–CPR5 or FUSE–SR45a–CPR5 and transferred them into the cpr5 mutant. Like RNPS1-N/CPR5-C,

these two fusion proteins can also complement the cpr5 mutant (Figure 3D). Among these fusion proteins, the best complementation of the cpr5 mutant is by SR45a-N/CPR5-C, which is consistent with the observation that the RRM domain of CPR5 is mostly similar to that of SR45a (Figure 3C; Supplemental Figure S3, D and E). Accordingly, the cpr5-induced expression of the defense genes PR1 and PR2 is suppressed largely by RNPS1-N/CPR5-C or SR45-N/CPR5-C and fully by SR45a-N/CPR5-C (Figure 3D). These data suggest that CPR5 is an RNA-binding protein of the Tra2 subfamily.

CPR5 and PRL1/FIP1 form a complex that localizes in nuclear speckles

In addition to the nuclear envelope, we clearly observed that CPR5 proteins were located in nuclear speckles (NSs; Wang et al., 2014; Gu et al., 2016), which was verified by observation of the CPR5–CFP fusion protein (Figure 4A). NSs are an RNA processing organelle, which is mainly enriched in pre-mRNA splicing factors, 3′-end RNA processing factors, and transcription factors (Lamond and Spector, 2003). However, we had no clue about the underlying biological significance of this subcellular localization and paid little attention to this unexpected localization since CPR5 was characterized as a nucleoporin (Gu et al., 2016). Now, our new findings about CPR5 protein functioning as an RNA-binding protein and as a component of RNA processing complex NTC/CPSF, make sense with the observation that it is a component of NSs (Figures 1–3 and 4A).

To dissect the underlying mechanism of how the SR family protein CPR5 regulates the NTC and CPSF RNA processing complexes, we explored the physical interactions between them. Since the full-length CPR5 protein is highly toxic to yeast, possibly due to the C-terminal TM domains, its N-terminus (1–339 aa) was used to perform yeast two-hybrid analysis. Our data show that CPR5 can interact with FIP1 in yeast (Figure 4B). We could not test the interactions with PRL1 in this system since it, fused with either activation domain or DNA-binding domain, exhibited strong autoactivation (Supplemental Figure S4A). We then conducted co-immunoprecipitation (co-IP) analysis to detect in vivo

Figure 3: (continued)
(AT1G07350), showing three putative domains including N-terminal SR domain, middle RRM and C-terminal TM domain. Bar = 100 aa. C, The putative RRM domain. Alignment of CPR5 and SR45a proteins using ClustalX2. RRM contains two highly conserved short-sequence motifs known as RNP1 (RNP octamer) and RNP2 (RNP hexamer). The RNP1 and RNP2 consensus sequences are (R/K)-G-(F/Y)-(G/A)-(F/Y)-V-X-(F/Y) and (L/I)-(F/Y)-(V/I)-X-(N/G)-L, respectively. The conserved aa residues are indicated (red dot). Plant species include dicots At, Glycine max (Gm), Gossypium arboreum (Ga), Rc, and Vitis vinifera (Vv); monocots Brachypodium distachyon (Bd), Oryza sativa Japonica Group (OsJ), Sorghum bicolor (Sb), Triticum dicoccoides (Td), and Zea mays (Zm). The cpr5 mutant allele, old1-3, in RNP2 is indicated. D, The SR-RRM domain swap test between CPR5 and RNPS1 (human) or SR45 or SR45a. Top: schematic diagram of the SR-RRM domain swap. The N-terminus of RNPS1 (1–240 aa, RNPS1-N), SR45 (1–176 aa, SR45-N) and SR45a (1–131 aa, SR45a-N), including SR and RRM domains, were used to replace the putative N-terminal SR-RRM domain of CPR5 (1–168 aa, CPR5-N) and fused to the C-terminus of CPR5 (169–564 aa, CPR5-C), referred to as FUSE-RNPS1-CPR5, FUSE-SR45-CPR5, and FUSE-SR45a-CPR5, respectively. Bottom left: 21-day-old WT, cpr5, cpr5/CPR5-C (CPR5-C), cpr5/RNPS1-N (RNPS1-N), cpr5/RNPS1 (RNPS1), cpr5/FUSE-RNPS1-CPR5 (RNPS1-CPR5), cpr5/FUSE-SR45-CPR5 (SR45-CPR5), and cpr5/FUSE-SR45a-CPR5 (SR45a-CPR5) plants were photographed for early senescence (arrows). Bottom right: qPCR was carried out on PR1 and PR2 in 21-day-old WT, cpr5, RNPS1-CPR5, SR45-CPR5, and SR45a-CPR5 plants. Total RNA was extracted from a mixture of T2 plants (six independent transgenic lines per construct). ACT2 was used as an internal control. Error bars represent SES. Experiments were conducted in triplicate. The letter above the bar indicates a statistically significant difference between groups at $P < 0.01$.
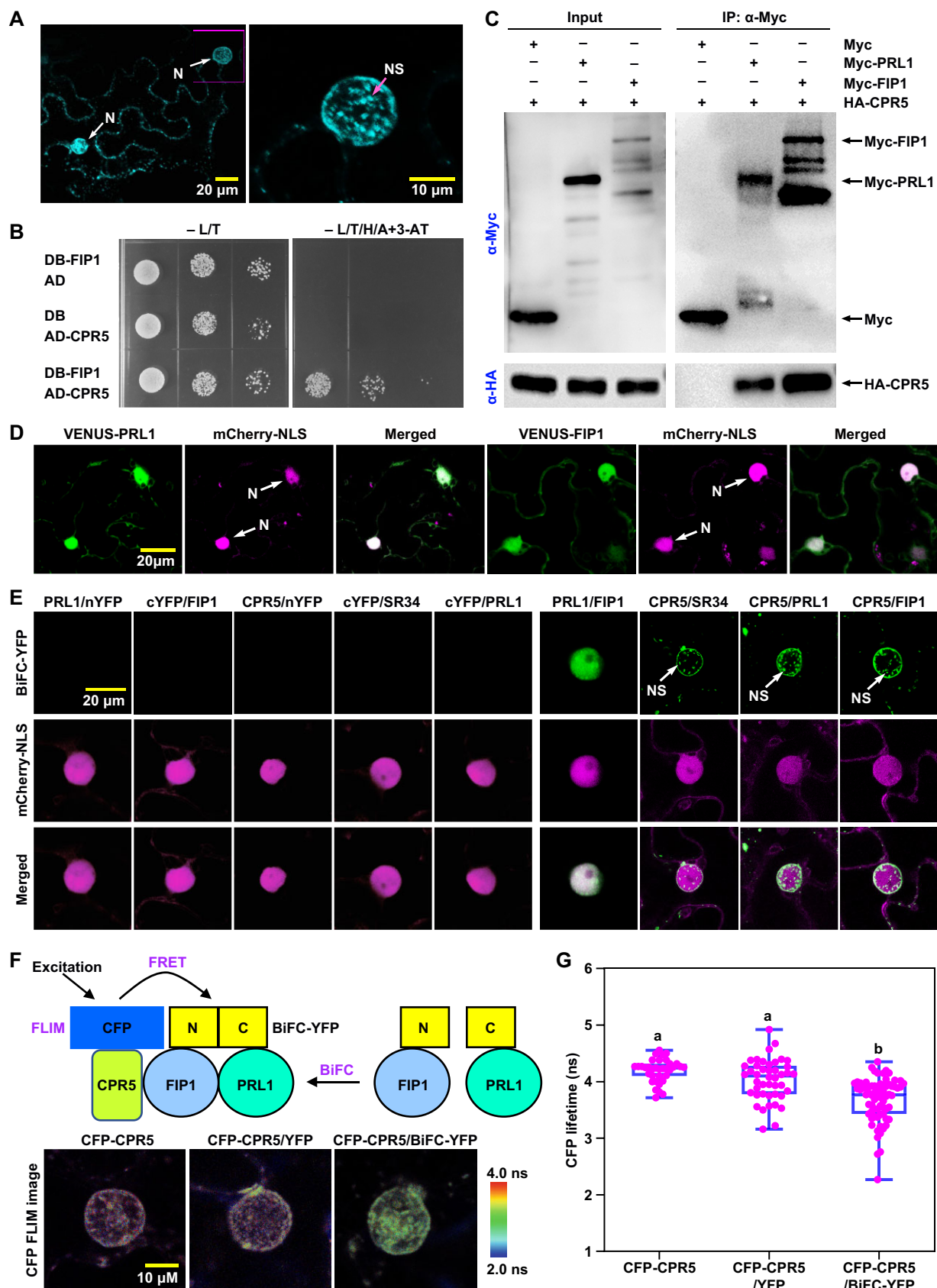
Figure 4 CPR5 interacts and colocalizes with PRL1 and FIP1. A, Subcellular localization of CPR5 protein. *Agrobacteria* carrying the construct of *35S:CFP-CPR5* (the *CFP–CPR5* fusion gene is driven by the *35S* promoter) was infiltrated into *N. benthamiana*. The magenta box in the left indicates the nucleus which is enlarged on the right. N, nucleus . B, The interaction between CPR5-N (N-terminus, 1–339 aa) and FIP1 was tested using yeast two-hybrid system. AD, yeast GAL4 activation domain; DB, yeast GAL4 DNA-binding domain. −L/T, SD base with leucine/tryptophan dropout supplement; −L/T/H/A + 3-amino-1,2,4-triazole (3-AT), SD base with leucine/tryptophan/histidine/adenine dropout supplement and

interaction between CPR5 and PRL1/FIP1. Hemagglutinin (HA)-tagged CPR5 was transiently co-expressed with Myc-tagged PRL1 or FIP1 in *Nicotiana benthamiana*. Our co-IP data demonstrated that CPR5 can be immunoprecipitated (IPed) by both PRL1 and FIP1, indicating that CPR5 can form a complex with PRL1/FIP1 in planta (Figure 4C).

As shown in Figure 4D, we generated the translational fusion proteins of PRL1 and FIP1 with VENUS (*PRL1:PRL1-VENUS* and *FIP1:FIP1-VENUS*) and found that PRL1 and FIP1 are both located in the nucleus. Bimolecular fluorescence complementation (BiFC) with split yellow fluorescent protein (BiFC-YFP) assays confirmed that PRL1 interacts with FIP1 in the nucleus (Figure 4E). These interactions were also verified using BiFC with split luciferase (BiFC-LUC) assay (Supplemental Figure S4B).

The typical SR superfamily proteins are well characterized as pre-mRNA splicing regulators and often used as subcellular markers to indicate NSs (Valcarcel and Green, 1996). Arabidopsis has at least 19 members of the SR superfamily, which are classified into seven subfamilies (Kalyna and Barta, 2004). We first performed a BiFC-LUC assay on seven of them (one from each subfamily) in *N. benthamiana* and found that CPR5 could strongly interact with SERINE/ARGININE-RICH PROTEIN SPLICING FACTOR 34 (SR34; AT1G02840) and RS-CONTAINING ZINC FINGER PROTEIN 22 (AT4G31580) (Supplemental Figure S4C). We then carried out a BiFC-YFP assay and found that CPR5 co-localized with SR34 to both nuclear envelope and NSs in *N. benthamiana*, validating that CPR5 is an NS protein, in addition to being a nucleoporin (Figure 4E; Gu et al., 2016). The BiFC-YFP assay further detected the interactions between CPR5 and PRL1 as well as CPR5 and FIP1, which appear in both nuclear envelope and NSs (Figure 4E).

On the basis of the BiFC-YFP assay (split-YFPs fused to the first two proteins FIP1-nYFP and cYFP-PRL1), Förster resonance energy transfer measured by fluorescence lifetime microscopy (FRET-FLIM) was performed to detect the transfer of excitation energy from CFP (fused to the third protein CPR5, CFP–CPR5) to BiFC-YFP (PRL1/FIP1) to test if these three proteins co-exist in a single complex. As compared to those of the negative controls, CFP–CPR5 alone and CFP–CPR5/YFP together, the CFP lifetime of CFP–CPR5/BiFC-YFP was significantly reduced (versus CFP–CPR5 alone, P-value = 5.33812E-11; versus CFP–CPR5/YFP, P-value = 5.42941E-06), which strongly indicates that CPR5 and PRL1/FIP1 can form a single ternary complex (Figure 4, F and G; Supplemental Figure S4D). Taken together, these data reveal a CPR5/PRL1/FIP1 complex which is localized to both nuclear envelope and NSs.

Regulation of pre-mRNA splicing and polyadenylation by CPR5

RNA-seq analysis was conducted for genome-wide profiling of pre-mRNA splicing and polyadenylation. In this analysis, we identified 3,104 DEGs (*cpr*5 versus WT, FC > 2, $P < 0.05$) (Supplemental Data Set 2A). The results show that there are 1,244 AS events (ASEs) which are significantly different between WT and *cpr*5 plants ($P < 0.05$) (Supplemental Data Set 2B). There are nine types of CPR5-regulated ASEs and the majority (83.1%) are composed of intron retention (IR) (46.1%), alternative 3'-splice site (A3SS, 22.5%) and alternative 5'-splice site (A5SS, 14.5%; Figure 5A; Supplemental Data Set 2B). It has been reported that there are 546 ASEs that are significantly different between WT and flg22-treated plants ($P < 0.001$). Accordingly, the majority of flg22-regulated ASEs (98%) are also composed of IR (85%), A3SS (7%), and A5SS (6%; Bazin et al., 2020). Among IR-type ASEs which presumably result in truncated proteins, the number of downregulated (DN) ASEs (379) is almost double that of UP ASEs (194), which is consistent with that most of *cpr*5-induced DEGs (72.78%) are UP (Figure 5A; Supplemental Data Set 1A). There are 473 alternative spliced genes (ASGs) associated with 1,244 CPR5-regulated ASEs (Supplemental Data Set 2B). Interestingly, the average transcript number per gene (6.64 ± 0.24) of CPR5-regulated ASGs is significantly more than that (2.40 ± 0.01) of all

Figure 4: (continued)
10 mM 3-AT. C, Co-IP was carried out by transiently co-expressing the Myc empty vector (*Myc*), Myc-tagged PRL1 (*Myc-PRL1*), or Myc-tagged FIP1 (*Myc-FIP1*) with HA-tagged CPR5 (*HA-CPR5*) in *N. benthamiana*. Protein extracts were IPed with α-Myc and resolved by SDS–PAGE. Input and IPed proteins were detected with both α-Myc and anti-HA antibody (α-HA). D, Subcellular localization of PRL1 and FIP1 proteins. *Agrobacteria* carrying the constructs of *35S:VENUS-PRL1* (VENUS fused to the N-terminus of PRL1) and *35S:VENUS-FIP1* as well as *35S:mCherry-NLS* (mCherry-NLS, the nuclear localization signal of SV40 protein fused to the C-terminus of mCherry) were co-infiltrated into *N. benthamiana*. mCherry-NLS was used as a marker of nucleus. E, BiFC assay was performed by transiently co-expressing *35S:mCherry-NLS*, *35S:cYFP-CPR5* (the C-terminus of yellow fluorescent protein fused to the N-terminus of CPR5) or *35S:cYFP-PRL1* with *35S:SR34-nYFP* (the N-terminus of YFP fused to the C-terminus of SR34) or *35S:PRL1-nYFP* or *35S:FIP1-nYFP* in *N. benthamiana*. mCherry-NLS and SR34 were used as markers of nucleus and NS, respectively. The empty vectors of *35S:nYFP* and *35S:cYFP* were used as negative controls. "/" is used to separate each pair of split-YFPs (cYFP alone or fusion protein/nYFP alone or fusion protein). For instance, PRL1/FIP1 stands for *cYFP-PRL1/FIP1-nYFP*. F, Top: Schematic diagram of the FRET-FLIM assay for detecting the CPR5/PRL1/FIP1 ternary complex. The transfer of excitation energy from CFP to a functional YFP formed from the split-YFPs (N, nYFP; C, cYFP) to generate FRET. The CFP lifetime is detected by FLIM. Bottom: The fluorescence lifetime heat maps. This assay was carried out by transiently expressing *35S:CFP-CPR5* alone (CFP-CPR5) or co-expressing *35S:CFP-CPR5* with either *35S:YFP-NLS* (the nuclear localization signal of SV40 protein fused to the C-terminus of YFP) (CFP-CPR5/YFP) or *35S:cYFP-PRL1/35S:FIP1-nYFP* (CFP-CPR5/BiFC-YFP) in *N. benthamiana*. Both CFP-CPR5 and CFP-CPR5/YFP are used as negative controls. Scale bar, CFP lifetime (ns, nanosecond). G, Box plot represents quantification of the CFP lifetime in Figure 4F. Experiments were conducted 3 times with similar results (*n* = 30–80). The letter above the bar indicates a statistically significant difference between groups at $P < 0.01$.
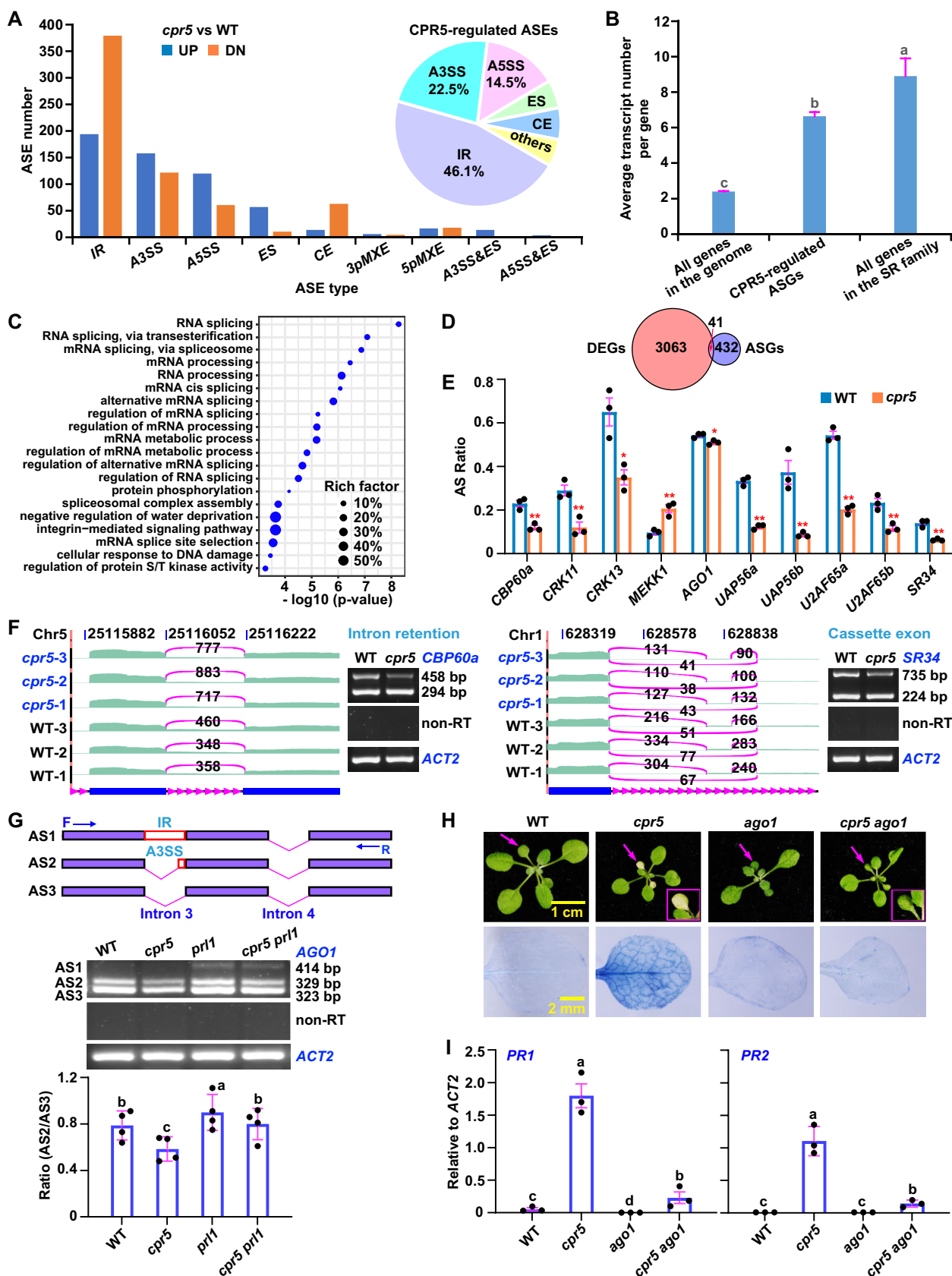
Figure 5 Genome-wide profiling of CPR5-regulated ASGs. A, Twelve-day-old WT and *cpr5* plants were used to perform RNA-seq analysis. RNA-seq data are available in the SRA database under the Bioproject accession number PRJNA737012. The *y*-axis represents the numbers of CPR5-regualted alternative spliced events (ASEs) (*cpr5* versus WT, $P < 0.05$), either UP or DN. There are nine types of ASEs: 3pMXE, 5pMXE, A3SS, A5SS, CE, ES, IR, A3SS&ES and A5SS&ES. Inset: pie chart shows the composition of nine types of CPR5-regualted ASEs. Experiments were carried out in triplicate. B, The average transcript number per gene of all genes in Arabidopsis genome (AtRTD2, 82,184 transcripts/34,211

genes in Arabidopsis genome (AtRTD2) (P = 1.96E-230; Figure 5B; Zhang et al., 2017a, 2017b).

SR proteins are RNA splicing regulators. Notably, human SR superfamily genes are highly alternatively spliced (Lareau et al., 2007). We therefore compared Arabidopsis SR family genes to all genes in the Arabidopsis genome and found that the SR superfamily genes are also highly alternatively spliced as their average transcript number per gene is 8.89 ± 1.00 (P = 8.60E-25; Figure 5B; Kalyna and Barta, 2004). GO enrichment analysis found that CPR5-regulated ASGs (473) are mostly enriched in RNA splicing regulators (P = 4.19E-09), which is the same as that in flg22-regulated ASGs (Figure 5C; Supplemental Data Set 2C; Bazin et al., 2020). The overlap between CPR5-regulated DEGs and ASGs is very low (8.67%; 41/473 ASGs), suggesting that CPR5 affects different set of genes in terms of RNA transcription and AS (Figure 5D; Supplemental Data Set 2, A and C). Taken together, these data reveal that CPR5 plays a critical role in RNA splicing.

The representative ASGs include SR34, U2AF65a, U2AF65b, UAP56a, UAP56b, ARGONAUTE 1 (AGO1), MAPK/ERK KINASE KINASE 1 (MEKK1), CALMODULIN-BINDING PROTEIN 60a (CBP60a), CYSTEINE-RICH RECEPTOR-LIKE PROTEIN KINASE 11 (CRK11), and CRK13 (Figure 5E). The ASEs of CBP60a and SR34, representing IR and non-IR (NIR), respectively, were validated by reverse transcription–polymerase chain reaction (RT–PCR;

Figure 5F). It has been reported that ASEs of the two NLR genes, SNC1 and RPS4, are regulated by the mediators of the SNC1 signaling pathway including the NTC component MOS12 and the SR protein transporter MOS14 (Xu et al., 2011, 2012). Our RT–PCR results showed that the expression of IR of both SNC1 and RPS4 is DN in cpr5 mutants but UP in prl1 fip1 mutants, validating that CPR5 and SNC1 share a common downstream immune signaling pathway (Supplemental Figure S5A).

We further characterized one of these ASGs, AGO1. AGO1 is an RNA-guided RNA endonuclease (Baulcombe, 2004). Around the third intron, we identified three ASEs, including an IR ASE (AS1), the typical ASE (AS2) and an A3SS ASE (AS3), in the AGO1 gene. RT–PCR analysis showed that the ratio of AS2/AS3 in cpr5 mutants is significantly lower than that in WT plants, which is consistent with that of RNA-seq analysis (Figure 5G; Supplemental Figure S5, B and C). To explore the epistatic interaction, we first generated a clustered regularly interspaced short palindromic repeats (CRISPR)/Cas9-edited ago1 mutant and then crossed it with cpr5 to obtain cpr5 ago1 double mutant. Intriguingly, the cpr5-induced early senescence and immune response are both suppressed by ago1, suggesting that AGO1 functions downstream of CPR5 to activate plant PCD and immunity (Figure 5, H and I).

We then performed polyadenylation site sequencing (PAS-seq) analysis to explore APA events (APAEs) between WT

Figure 5: (continued)

genes), CPR5-regulated ASGs (3,126 transcripts/472 genes) and SR family genes (169 transcripts/19 genes). The letter above the bar indicates a statistically significant difference between groups at P < 0.01. C, GO enrichment analysis of CPR5-regulated ASGs (P < 0.05). The bubble chart shows biological process enrichment of these genes. The y-axis represents biological process. The x-axis represents the enrichment significance (−log10 P-value). Size of the bubble represents rich factor, which is the ratio of the amount of CPR5-regulated ASGs enriched in a biological process and the amount of all genes annotated in this biological process. D, Venn diagram proportionally shows the overlap between CPR5-regulated 3,104 DEGs (cpr5 versus WT, FC > 2, P < 0.05) and 473 ASGs (cpr5 versus WT, P < 0.05). E, Bar graph depicting the AS ratio of ASGs determined by RNA-seq analysis. The representative ASGs include RNA splicing regulators SR34 (AT1G02840), U2AF65a (AT4G36690), U2AF65b (AT1G60900), UAP56a (AT5G11170), and UAP56b (AT5G11200), and plant immune regulators AGO1 (AT1G48410), MEKK1 (AT4G08500), CBP60a (AT5G62570), CRK11 (AT4G23190), and CRK13 (AT4G23210). ASEs are divided into two groups: IR and NIR. The AS ratio is calculated using the formula: for IR ASEs, intron reads/exon reads; for NIR ASEs, AS1 reads/(AS1 reads + AS2 reads). Experiments were carried out in triplicate. Statistical significance of the AS ratio difference between WT and cpr5 was determined by t test and indicated by asterisks: *P < 0.05 and **P < 0.01. F, Read coverage of the representative ASGs. Sashimi plots of RNA-seq data showing the sequencing read coverage of CBP60a on chr5 (left) and SR34 on chr1 (right), representing IR and CE, respectively, in WT and cpr5 samples. The genomic coordinates for each splicing event are shown at the top and the schematic diagram of this splicing event is shown at the bottom. The number in each line represents the reads spanning each exon junctions. Experiments were carried out in triplicate. The splicing patterns of these genes in WT and cpr5 plants were validated by RT-PCR. PCR was performed on RT products (DNase-treated total RNA incubated with reverse transcriptase) for CBP60a, SR34, and ACT2. ACT2 was used as an internal control. To check if genomic DNA was completely removed, PCR was also conducted on the DNase-treated total RNA (non-RT) for CBP60a and SR34. G, Splicing pattern of AGO1. Top: Schematic diagram of three ASEs (AS1, AS2, and AS3) around the third intron of the AGO1 gene. The fourth intron was included for distinguishing RT products from genomic DNA contamination. Middle and bottom: Total RNA was extracted from 12-day-old WT, cpr5, prl1, and cpr5 prl1 plants. Transcripts of AGO1 were determined by RT-PCR (middle) and quantified by ImageJ (https://imagej.nih.gov/ij/) (bottom). PCR was performed on RT products for AGO1 and ACT2. ACT2 was used as an internal control. To check if genomic DNA was completely removed, PCR was conducted on non-RT for AGO1. The size of PCR products: AS1 = 414 bp, AS2 = 329 bp, and AS3 = 323 bp. F, forward primer AGO1-AS-F; R, reverse primer AGO1-AS-R. Experiments were conducted in four replicates. The letter above the bar indicates a statistically significant difference between groups at P < 0.01. H, Top: 21-day-old WT, cpr5, ago1 (the CRISPR/Cas9-edited mutant), and cpr5 ago1 plants were photographed for early senescence (arrows). Insets: the arrow-pointed leaves of cpr5 and cpr5 ago1 are enlarged. Bottom: true leaves of 12-day-old WT, cpr5, ago1, and cpr5 ago1 plants were stained with Trypan blue for cells that had undergone PCD. I, qPCR was carried out on PR1 and PR2 in 18-day-old WT, cpr5, ago1 and cpr5 ago1 plants. ACT2 was used as an internal control. Error bars represent SEs. Experiments were conducted in triplicate. The letter above the bar indicates a statistically significant difference between groups at P < 0.01.
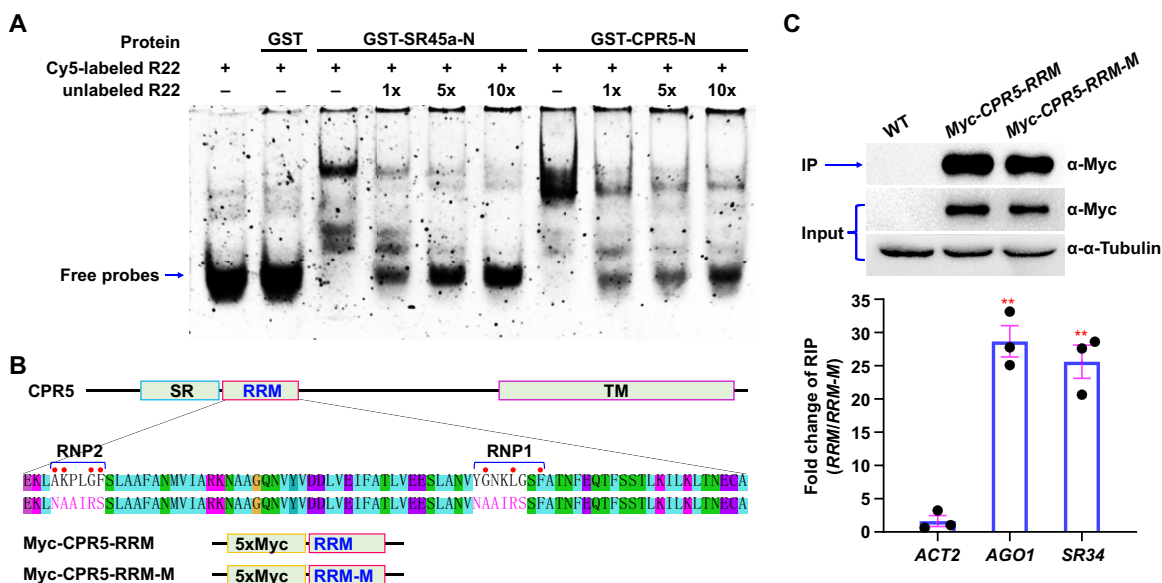
Figure 6 The RNA-binding assay of CPR5 protein. A, REMSA was carried out for detecting RNA–protein interaction. Cy5-labeled RNA probes (5 nM, human Tra2-targeted RNA sequence R22), together with or without unlabeled probes, were incubated with GST-tagged proteins (2.5 μg) and resolved by a native polyacrylamide gel. The unlabeled probes (competitors) were added in an increasing concentration gradient, including 5 nM (1×), 25 nM (5×), and 50 nM (10×). GST, GST-tagged N-terminus of CPR5 (GST-CPR5-N, 1–191 aa, including the SR-RRM domain) and GST-tagged N-terminus of SR45a (GST-SR45a-N, 1–151 aa, including the SR-RRM domain), were obtained from E. coli. GST and GST-SR45a served as negative and positive controls, respectively. B, Schematic diagram of the Myc-tagged proteins. The putative RRM (113–191aa) of CPR5 protein (Myc-CPR5-RRM) was used for RIP analysis. The mutation of Myc-CPR5-RRM (Myc-CPR5-RRM-M), in which both RNP1 and RNP2 in Myc-CPR5-RRM were replaced with a linker NAAIRS, served as a mock control. C, Top: 18-day-old WT, Myc-CPR5-RRM and Myc-CPR5-RRM-M transgenic plants were used to perform RIP analysis. WT was used as a negative control. Total proteins (Input) were blotted with anti-α-Tubulin (α-α-Tubulin) and anti-Myc (α-Myc). The IPed proteins were blotted with α-Myc. Bottom: qPCR was conducted on AGO1 and SR34 in the RIP samples. ACT2 was used as a negative control. The FC is the RIP ratio of Myc-CPR5-RRM/Myc-CPR5-RRM-M (RRM/RRM-M). Error bars represent SEs. Experiments were conducted in triplicate. **, indicates a statistically significant difference of FC (AGO1 vs ACT2 or SR34 vs ACT2) at $P < 0.01$.

and cpr5 plants. APAEs are categorized into two groups: longer termination (LT) and shorter termination (ST). PAS-seq analysis shows that there are 103 LTs and 40 STs that are significantly different between WT and cpr5 plants ($P < 0.05$). These APAEs, both LT and ST, are associated with 84 genes, designated as alternative polyadenylated genes (APAGs) (Supplemental Data Set 2D). Read coverages of the representative APAGs with significant differences between WT and cpr5 plants ($P < 0.05$) such as Cwf18 (AT3G05070), encoding an RNA splicing regulator, and DABB1 (AT1G51360), encoding an immune regulator, are shown in Supplemental Figure S5D. There are 1,244 CPR5-regulated ASEs ($P < 0.05$), whereas there are only 143 CPR5-regulated APAEs ($P < 0.05$), suggesting that the CPR5-NTC/CPSF signaling pathway is mainly involved in regulation of AS but not APA and the CPSF complex may be recruited by the NTC complex to regulate AS (Supplemental Data Set 2, B and E).

It appears that the CPR5-NTC/CPSF signaling pathway affects different sets of genes in terms of RNA transcription, splicing, and polyadenylation. The overlaps between CPR5-regulated DEGs, ASGs and APAGs are very limited as the overlaps between DEGs and ASGs, DEGs and APAGs, and

ASGs and APAGs are 8.67% (41/473 ASGs), 4.76% (4/84 APAGs), and 2.38% (2/84 APAGs), respectively (Figure 5D; Supplemental Figure S5E; Supplemental Data Set 2E). CPR5 is an RNA-binding protein but not a transcription factor. Presumably, the CPR5-NTC/CPSF signaling pathway alters the ratio of alternatively spliced transcripts (ASTs) but not the total expression of an ASG. Meanwhile, some of the CPR5-regulated ASGs/APAGs are transcription factors that mediate CPR5 signaling and alter the expression but not the ratio of ASTs of their targeted DEGs, which could be a different set of genes from ASGs/APAGs.

The RNA-binding activity of CPR5 protein

In terms of the RRM domain, CPR5 is mostly close to SR45a, which is an Arabidopsis homolog of human Tra2 (Supplemental Figure S3, D and E). Human Tra2 binds the oligo (GAA)-containing RNA sequence, which functions as a splicing enhancer (Tacke et al., 1998). Therefore, we tested if CPR5 could directly bind human Tra2-targeted RNA sequence. A well-characterized human Tra2-targeted RNA sequence R22 (AAAGAACAAGAAGAAGAAG) was used for RNA electrophoretic mobility shift assay (REMSA; Tacke et al., 1998). R22 was synthesized and labeled with Cyanine-

5 (Cy5) at the 5′-end. Glutathione-S-transferase (GST)-tagged SR-RRM domains of SR45a (1–151 aa; GST-SR45a-N) and CPR5 (1–191 aa; GST-CPR5-N) were obtained from *Escherichia coli*. SR45a and GST were used as positive and negative controls, respectively. As expected, SR45a proteins could bind R22, whereas GST itself could not bind R22. Amazingly, CPR5 proteins could bind Cy5-labeled R22 probes, which were fully competed by excessive unlabeled ones, confirming that CPR5 protein is an RNA-binding protein of the Tra2 subfamily (Figure 6A).

To investigate if the putative RRM domain of CPR5 protein (113–191 aa) is capable of in planta binding RNAs of the CPR5-regulated ASGs identified by RNA-seq analysis, we performed RNA immunoprecipitation (RIP). The Myc-tag was fused to the N-terminus of CPR5 RRM domain to generate Myc-CPR5-RRM. The two short consensus sequences RNP1 and RNP2 in Myc-CPR5-RRM were replaced with a flexible linker asparagine–alanine–alanine–isoleucine–arginine–serine (NAAIRS) to generate Myc-CPR5-RRM-M, which served as a mock control (Figure 6B). Presumably, the NAAIRS substitution has little damage to the structure of the peptide (Wilson et al., 1985). We first checked if Myc-tagged proteins were IPed by anti-Myc magnetic beads. The results showed that these Myc-tagged proteins are present in both total proteins and IPed proteins and the sizes of fusion proteins are as expected (19.86 kDa). FC was calculated by the IPed transcripts of Myc-CPR5-RRM sample over those of Myc-CPR5-RRM-M sample (Myc-CPR5-RRM/Myc-CPR5-RRM-M), which were quantified by qPCR. As compared to those of the negative control ACTIN 2 (ACT2) (FC = 1.39 ± 1.53), the transcripts of two ASGs, AGO1 (FC = 25.69 ± 5.07) and SR34 (FC = 20.60 ± 3.55), were significantly enriched by RIP, indicating that CPR5 proteins can bind the transcripts of AGO1 and SR34 in planta, which may lead to the differential AS of these genes (Figure 6C).

Discussion

The regulation of plant immune plasticity in response to infections of largely diverse and ever evolving pathogens is so sophisticated that it requires coordination of multiple fundamental signaling pathways such as DNA epigenetic modification, RNA processing, and protein–protein interaction (Staiger et al., 2013; Bohm et al., 2014; Ramirez-Prado et al., 2018). Although the flexibility of RNA splicing and polyadenylation has long been implicated in plant immunity, the underlying regulatory mechanism of this process remains largely unclear. CPR5 is a key negative regulator of plant immunity. Previously, CPR5 was characterized as a nucleoporin and controls plant immunity through nuclear transportation and cell cycle progression (Wang et al., 2014; Gu et al., 2016). This study further reveals that CPR5 is an RNA-binding protein belonging to the SR family and modulates plant immunity via the two RNA processing complexes, NTC and CPSF, which may provide inexhaustible resources for boosting plant immune plasticity.

CPR5 is a novel RNA-binding protein belonging to the SR family

CPR5 was first identified as a negative immune regulator (Bowling et al., 1997). Lack of the function-known domain of this protein has been an obstacle to advance our understanding of its regulatory mechanism. In this study, we characterized CPR5 as an RNA-binding protein belonging to the Tra2 subfamily of SR family based on the feature of SR-RRM domain structure. Most strikingly, the putative RRM domain of CPR5 protein can be functionally substituted by those of Tra2 subfamily proteins, including human RNPS1 as well as Arabidopsis SR45 and SR45a (Figure 3; Supplemental Figure S3). Accordingly, the RRM domain of CPR5 can bind human Tra2-targeted RNA sequence in vitro and bind RNAs of CPR5-regulated ASGs such as SR34 and AGO1 in planta (Figure 6). Typically, SR proteins contain an RRM-SR domain structure. On the contrary, Tra2 subfamily proteins possess an SR-RRM domain structure, indicating that it is an atypical subfamily in the SR superfamily (Califice et al., 2012). CPR5 protein is a nucleoporin and has 4–5 TM domains (Wang et al., 2014; Gu et al., 2016). Neither nucleoporin nor TM domain has been identified in the SR superfamily, suggesting that CPR5 is a novel RNA-binding protein of this family (Califice et al., 2012).

SR superfamily proteins play a central role in RNA processing, such as transcription, 5′-end capping, 3′-end polyadenylation, splicing, transportation, and translation (Califice et al., 2012). Tra2 and RNPS1 are two members of Tra2 subfamily. Based on the RRM domain, Arabidopsis SR45 and SR45a are homologs of human RNPS1 and Tra2, respectively (Supplemental Figure S3, D and E; Califice et al., 2012). Tra2 protein controls the AS of Doublesex, which plays a pivotal role in sex determination in Drosophila melanogaster (Hoshijima et al., 1991). RNPS1 is a general pre-mRNA splicing activator which is a component of the apoptosis- and splicing-associated protein complex in human (Deka and Singh, 2017). Arabidopsis SR45 was identified as a negative regulator of plant immunity as sr45 mutants exhibited enhanced resistance to the bacterial pathogen Psm ES4326 as well as to the oomycete Hpa Noco2 (Zhang et al., 2017a, 2017b). Arabidopsis SR45a was reported to regulate AS of the salt-stress response genes (Li et al., 2021). These findings demonstrate that Tra2 subfamily proteins function as RNA splicing factors and regulate biotic and abiotic stress responses in plant.

As an SR family protein, CPR5 complexes with RNA processing regulator NTC/CPSF and is located in NSs, strongly suggesting that CPR5 play a role in RNA processing (Figures 1–4; Supplemental Figures S1–S4; Supplemental Table S1; Supplemental Data Set 1). Consistently, RNA-seq analysis reveals that there is a significant difference of AS between WT and cpr5 plants. Interestingly, AGO1 is one of the CPR5-regulated ASGs (Figure 5; Supplemental Figure S5; Supplemental Data Set 2). Consistently, RIP analysis confirms that CPR5 can bind AGO1 RNA in planta (Figure 6). The AGO family protein functions as an RNA-guided RNA endonuclease and is a core component of the RNA-induced

silencing complex (Baulcombe, 2004). Arabidopsis NTC proteins, including Aquarius, PRL1 and Prp19, are required for primary-microRNA (miRNA) accumulation (Jia et al., 2017). In addition to cleaving the targeted nucleic acids, AGO1 also regulates miRNA accumulation (Reichholf et al., 2019). The *ago1* mutants are less sensitive to flg22-treatment than WT plants and consistently AGO1 is required for flg22-induced plant resistance to *P. syringae* (Li et al., 2010). These data suggest that CPR5 globally controls AS of immune genes, such as *AGO1*, to regulate plant immunity.

The NTC and CPSF RNA processing complexes coordinately regulate plant immunity

The interplay between RNA splicing and polyadenylation has been implicated in diverse biological processes (Elkon et al., 2013). The active 3′-end polyadenylation factor CPSF is required for the splicing of a single-intron pre-mRNA, whereas mutation of the AAUAAA sequence in a multi-intron pre-mRNA inhibit the splicing of the 3′-terminal intron but not the internal introns. Direct interaction between the spliceosome component U2 and CPSF helps enhance 3′-end processing. Genome-wide analysis identified a large number of CPSF100-binding peaks in coding regions and introns within the mRNA (Misra et al., 2015; Misra and Green, 2016). Although it has been known for years that NTC mediates the SNC1 signaling pathway and CPSF30 regulates SA-dependent PCD and immunity, whether and how the interplay between RNA processing complexes regulates plant immunity remains unknown (Palma et al., 2007; Monaghan et al., 2009; Bruggeman et al., 2014).

Our genetic study discovered that both NTC and CPSF function downstream of CPR5. Epistatic interaction analysis further reveals that these two RNA processing complexes coordinately regulate plant immunity and PCD (Figures 1 and 2; Supplemental Figures S1 and S2). BiFC analyses confirm that PRL1 and FIP1 form a complex which is colocalized in nucleus (Figure 4; Supplemental Figure S4). Interestingly, both CPR5-regulated and flg22-induced ASGs are mostly enriched in RNA splicing regulators (*P* = 4.19E-09) (Figure 5C; Supplemental Data Set 2C; Bazin et al., 2020). It appears that CPR5-regulated ASGs are alternatively spliced hotspots as the average transcript number per gene of CPR5-regulated ASGs is significantly more than that of all genes in Arabidopsis genome (AtRTD2) (*P* = 1.96E-230; Figure 5B). Genome-wide RNA profiling showed that there are many more ASGs (473) than APAGs (84) regulated by CPR5, suggesting that CPR5 preferably mediates AS and CPSF may be recruited by NTC to facilitate AS during immune response (Figure 5; Supplemental Figure S5; Supplemental Data Set 2E). These findings reveal a very interesting yet poorly understood phenomenon that RNA splicing regulators are to alternatively splice themselves first and then the downstream genes to efficiently boost the signal complexity which may account for establishment of cellular homeostasis in response to the complex stresses.

CPR5 links nuclear transportation, cell cycle progression, and RNA processing together to control plant immunity

Previously, we discovered that CPR5 controls plant immunity and PCD through the CDK INHIBITOR (CKI)-RETINOBLASTOMA (RB)-E2F core cell cycle signaling pathway (Wang et al., 2014; Gu et al., 2016). There is a growing body of evidence to suggest that plant cell cycle progression is reprogrammed during plant–microbe interactions. For instance, infection of biotrophic pathogen is facilitated by induction of endoreduplication and plant ETI is often associated with PCD (Jones and Dangl, 2006; Wildermuth et al., 2017). It has been shown that the expression of NLR genes is regulated by cell cycle regulators ANAPHASE-PROMOTING COMPLEX/CYCLOSOME and MOS1(Bao et al., 2013; Zhang et al., 2018). However, downstream of NLRs, how cell cycle regulators are involved in plant immunity is still largely unknown. Usually, CPR5 binds the cell cycle regulator CKI. Upon pathogen infection, the activated NLRs successively release CKI from CPR5, trigger RB hyperphosphorylation and activate E2F, leading to heightened plant immunity and PCD (Wang et al., 2014; Gu et al., 2016).

Later, CPR5 was characterized as a nucleoporin associated with the selective barrier of NPC. The nuclear export receptor EXPORTIN-4 was recently found to be a genetic interactor of CPR5 (Xu et al., 2021). Activated NLR changes the conformation of CPR5 protein, which reconfigures the selective barrier to allow nuclear transportation of immune signals (Gu et al., 2016). Plant ETI requires nuclear accumulation of NLR proteins, such as barley mildew A, tobacco N receptor, and Arabidopsis RPS4 (Shen and Schulze-Lefert, 2007). EDS1 acts as a co-receptor of NLRs and the role of the EDS1/NLR/effector complex is determined by its subcellular localization as it triggers PCD in cytoplasm and ETI in nucleus (Bhattacharjee et al., 2011; Heidrich et al., 2011). Genetic dissection of the SNC1 signaling pathway found that members of the NPC, including Nucleoporin 96 (Nup96)/MOS3 and Nup88/MOS7, function downstream of NLR (Zhang and Li, 2005; Cheng et al., 2009). These findings indicate that nucleocytoplasmic transportation plays a pivotal role in plant immunity.

In this study, we further discovered that CPR5 is an RNA-binding protein and controls plant immunity via NTC and CPSF (Figures 1–6; Supplemental Figures S1–S5). CPR5 is located in both nuclear envelope and NSs (Figure 4). NS is a dynamic reservoir of RNA splicing regulators in a cell cycle-dependent manner (Lamond and Spector, 2003). The regulators stored in NSs are activated through phosphorylation by cell cycle regulator CDK. For instance, the core NTC component CDC5 is phosphorylated by CDK2 and RNPS1 is colocalized with the CDK11 in NSs (Graub et al., 2008; Loyer and Trembley, 2020). Therefore, the core cell cycle regulator CKI could be released from CPR5 to activate RNA processing regulators in NSs.
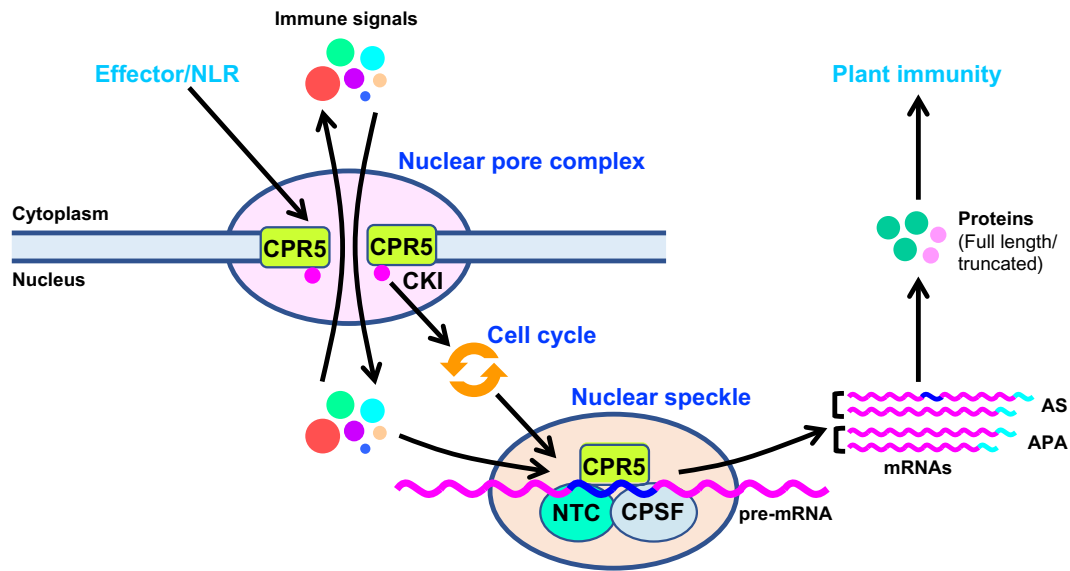
Figure 7 A proposed model of the CPR5-NTC/CPSF signaling pathway in plant immunity. CPR5 is a component of both NPC and NS. In the NPC, CPR5 inhibits the transportation of immune signals into nucleus and binds the cell cycle regulator CKI. In the NS, CPR5 binds the NTC/CPSF complex. Upon pathogen infection, immune signals enter nucleus and CKIs are released from CPR5, which together activate the NTC/CPSF complex. This activated NTC/CPSF complex regulates RNA processing, such as pre-mRNA AS and APA, leading to full length and truncated proteins. The ratio of full-length/truncated proteins may be determined to modulate plant immune plasticity against diverse and evolving pathogens.

Taken together, downstream of NLRs, CPR5 plays a central role linking nuclear transportation, cell cycle progression and RNA processing together to modulate plant immunity. A putative model of the CPR5-NTC/CPSF signaling pathway is shown in Figure 7. On the one hand, CPR5 functions as a component of NPC in nuclear envelope. Activated NLRs change the conformation of CPR5 protein to promote nuclear transportation of immune signals and release of cell cycle regulator CKIs. On the other hand, CPR5 functions as a component of RNA processing complex in NS. As an RNA-binding protein, CPR5 may determine the alternative spliced targets. CKIs, together with immune signals, promote release of RNA processing regulators, including NTC and CPSF, from CPR5. Activated RNA processing complex alternatively splices RNAs, leading to alternative transcripts which encode alternative proteins (isoforms). The plasticity, including specificity and intensity, of plant innate immunity is determined by the ratio of protein isoforms, such as full-length/truncated proteins. Therefore, our study on the CPR5-NTC/CPSF signaling pathway reveals, for the first time, that nuclear transportation, cell cycle progression, and RNA processing are integrated into a signaling hub, which orchestrates the perceiving of external stimuli and the reprogramming of internal responses.

Liquid–liquid phase separation (LLPS) has recently emerged as a general mechanism to form biomolecular condensates either originated from 2D membrane, such as NPC, or originated from 3D cytoplasm, such as NS. As demonstrated by the guanylate-binding protein-like GTPase defense-activated condensates, LLPS plays a pivotal role in plant immunity (Huang et al., 2021). LLPS is often driven by the multivalent RNA and RNA-binding proteins with low-complexity regions (LCRs) such as the SR domains (Calabretta and Richard, 2015). It is conceivable that CPR5 protein serves as a component of LLPS as it belongs to the SR family and is predicted to contain two LCRs (9–141 aa and 262–348 aa) by segmentation algorithm (SEG) (Wootton, 1994). Although membrane-bound and cytoplasmic LLPSs intimately interact with each other, it has not been found that a protein with TM domains is translocated between them (Snead and Gladfelter, 2019). How CPR5 protein is physically located in NSs and whether it is translocated between nuclear envelope and NS through LLPS during the immune response remains to be investigated since it possesses four to five TM domains in the C-terminus.

Materials and methods

Plant materials and growth conditions

Arabidopsis thaliana plants used in this study are in the Col-0 background. The *cpr5-1* (referred to as *cpr5*) mutant is as described (Bowling et al., 1997). Mutants of *prl1-T* (SALK_202998), *fip1-T* (SALK_099558), *mac3a* (SALK_089300), *mac3b* (SALK_074578), *cdc5* (SALK_074578), and *cpsf30* (SALK_049389) were obtained from ABRC. The condition of growth chamber was set temperature at 22°C and light intensity at 120 μmol m^{-2} s^{-1} generated by Philips Lifemax Cool White fluorescent bulbs with a 16-h light/8-h dark photoperiod.

Mutant screen and gene cloning

The *cpr5* seeds were mutagenized with EMS. The genetic screen for *scpr* mutants was carried out as described (Wang et al., 2014). The genes of *SCPR* candidates were cloned by

the combination of positional cloning and NGS. Positional cloning was used for rough mapping which located the gene in a big region on a chromosome, while NGS was carried out for fine mapping which identified SNPs of the whole genome. NGS was performed using Illumina NovaSeq 6000 at the Personal Biotechnology Co., Ltd. (Shanghai, China).

Trypan blue staining
Trypan blue staining was carried out as described (Wang et al., 2014).

qPCR
RNA was extracted using TRIzol Reagent (Invitrogen, Waltham, MA, USA) and cDNA was synthesized using the SuperScript III cDNA Synthesis (Invitrogen). qPCR was performed using NovoStart SYBR qPCR SuperMix plus (Novoprotein, Shanghai, China) in Mastercycler ep realplex (Eppendorf, New York, NY, USA). ACT2 (AT3G18780) was used as an internal control. Primers used for qPCR are listed in Supplemental Table S2.

Pathogen infection
Infection of Arabidopsis plants with Psm ES4326 with or without AvrRpt2 was carried out as previously described (Wang et al., 2014). Briefly, 4-week-old plants were ready for pathogen infection. Bacteria were streaked on King's B medium containing 100-μg/mL streptomycin and incubated at 30°C for 2 days. This step was repeated 2 times to revive the pathogen. To resuspend the pathogen, 10 mM $MgSO_4$ and four to six beads were added to the plate and gently shaken. The suspension was diluted with 10 mM $MgSO_4$ to a working solution (for instance, Psm ES4326, optical density at 600 nm (OD_{600}) = 0.0001). A blunt end 1-mL syringe was used to inject the suspension into the underside of leaves (2 leaves per plant, 12 plants per genotype). Bacterial counts in leaves were assessed on the day of the infection (Day 0) and 3 days after the infection (Day 3). Leaf disks (two leaf disks per plant, eight plants per genotype) were taken using a standard paper hole punch (diameter, 8 mm). Two leaf disks were placed in a 2-mL tube containing beads and 500 μL of 10 mM $MgSO_4$ and ground using Geno-Grinder. Twenty microliters of the tissue suspension was transferred to a 96-well plate containing 180 μL of 10-mM $MgSO_4$. A series of $10\times$ dilutions were conducted by transferring successive 20-μL portions of the preceding dilution to 180 μL of 10-mM $MgSO_4$. Rows of 10-μL aliquots were plated with an eight-channel pipette from each dilution onto King's B medium containing 100-μg/mL streptomycin. Plates were incubated at 30°C for ~2 days. The individual colonies growing on the most readable dilution were counted.

Ion leakage measurement
Psm ES4326/AvrRpt2-induced ion leakage was measured as previously described (Wang et al., 2014).

RNA-seq analysis
RNA-seq analysis was carried out at the Personal Biotechnology Co., Ltd. (Shanghai, China). In brief, total RNAs were extracted using the RNeasy Plant Mini Kit (Qiagen, Hilden, Germany). The RNA-seq libraries were constructed using the TruSeq RNA Sample Prep Kit (Illumina, San Diego, CA, USA). The mRNA was purified using oligo(dT) magnetic beads and then fragmented (~300 bp). The first-strand cDNA was synthesized with random hexamer primers. The double-strand cDNA was synthesized, ligated to the sequencing adaptors, and purified by AMPureXP beads. The fragments with adaptor were amplified by adaptor-specific primers, quantified by a Quantifluor-ST Fluorometer (Promega Madison, WI, USA) and a Quant-iT Picogreen dsDNA Assay kit (Invitrogen). The DNA library quality was tested by an Agilent 2100 Bioanalyzer (Agilent Technologies, Santa Clara, CA, USA) and an Agilent High Sensitivity DNA kit (Agilent Technologies). The libraries were applied to the Illunima HiSeq X Ten system for 150-nt paired-end sequencing. Three biological replicates were performed separately. For each sample, we obtained ~40 million raw reads. About 92% of them were useful clean reads after data filtration. The filtration steps were as follows: (1) remove reads containing only the adaptor sequences and (2) remove reads with average quantity lower than molecular quantity 20. About 96% of the useful reads could be uniquely mapped to the reference of A. thaliana TAIR10 using HISAT2 (http://ccb.jhu.edu/software/hisat2/index.shtml). At least 99.6% of the clean reads could be mapped to the exons, and ~99.0% clean reads could be mapped to genes. Gene annotation was referred to databases of Ensembl (http://www.ensembl.org/). Gene expression levels were normalized based on fragments per kilobase of exon model per million (FPKM) mapped fragments. DESeq was used for analyzing the significantly DEGs (FC > 2, $P < 0.05$).

Phylogenetic analysis
Phylogenetic tree was generated by Phylogeny.fr (Dereeper et al., 2008) (http://www.phylogeny.fr/simple_phylogeny.cgi). A text file of the alignment used to generate the phylogenetic tree is provided as Supplemental File S1.

Confocal laser scanning microscopy
BiFC-YFP was observed using an LSM 5 PASCAL Confocal Laser Scanning Microscope (Zeiss, Oberkochen, Germany) with the excitation wavelength at 514 nm and the emission wavelength between 525 and 570 nm. Based on the BiFC-YFP assay of protein–protein interaction (split-YFPs fused to the first two proteins), FRET-FLIM was performed to detect the transfer of excitation energy from CFP (fused to the third protein) to BiFC-YFP with a Leica STELLARIS8 confocal microscope (Fassler and Pimpl, 2017). CFP was excited by the 405-nm laser line and detected at 485 nm.

Yeast two-hybrid assay
The Matchmaker Gold Yeast Two-Hybrid System (Clontech, Mountain View, CA, USA) was used according to the

manufacturer's instructions. The coding DNA sequences were cloned into the pGBKT7 or pGADT7 vectors using the ClonExpressII One Step Cloning Kit (Vazyme Biotech, Nanjing, China). These constructs were transformed into *Saccharomyces cerevisiae* strain Y187 and Y2HGold. The diploid yeasts from the mating of these two strains were dropped on the media of synthetic defined (SD)-Leu/-Trp and SD–Leu/–Trp/–His/–Ade. Autoactivation assays were performed for each bait and prey construct with corresponding empty vector to exclude potential false positives.

Co-IP
Co-IP was conducted as described (Wang et al., 2014). Briefly, Myc-tagged proteins were transiently co-expressed with HA-tagged proteins in *N. benthamiana*. Protein extraction buffer consists of 50 mM Tris (pH 7.5), 150 mM NaCl, 1% Triton X-100, 5 mM β-mercaptoethanol, 1-mM phenylmethanesulfonyl fluoride and Protease Inhibitor Cocktail (Cat. No. P1015; Beyotime, Shanghai, China). Protein was IPed with anti-Myc antibody (α-Myc; Cat. No. AF6513, Beyotime) and resolved by sodium dodecyl sulfate–polyacrylamide gel electrophoresis (SDS–PAGE). Input and IPed proteins were detected with both α-Myc and anti-HA antibody (α-HA; Cat. No. AF0039; Beyotime).

The CRISPR/Cas9 editing system
The vector of *pCas9-T1* (GenBank accession number MZ476947) was derived from *pEarleyGate 100*. The CRISPR-associated endonuclease Cas9 was from the *Streptococcus pyogenes*, which was driven by Arabidopsis *YAO* (AT4G05410) promoter. The DNA-targeting CRISPR RNA of single-guide RNA sequence was designed using the CRISPR/Cas9 target online predictor (CCTop) (https://cctop.cos.uni-heidelberg.de/) (Stemmer et al., 2015) and driven by Arabidopsis *U6-26* (AT3G13855) promoter. Transgenic plants were sequenced for homozygous edited mutations.

BiFC assays
BiFC-LUC or BiFC-YFP assays were carried out as described (Wang et al., 2014).

RNA AS analysis
RNA AS analysis was conducted at the Wuhan Ruixing Biotechnology Co., Ltd (Wuhan, China). Total RNA was treated with RQ1 DNase (Promega). The RNA-seq libraries were constructed using the NEBNext Ultra Directional RNA Library Prep Kit (Illumina). Briefly, polyadenylated mRNAs were purified, fragmented, and converted into double-strand cDNA. After end-repair and dA-tailing, the DNAs were ligated to the NEBNext Adaptor and digested with heat-labile uracil-DNA glycosylase. The libraries were applied to the Illumina HiSeq X Ten system for 150-nt paired-end sequencing. Among the raw sequencing reads, those containing more than 2-N bases and those <16-nt were discarded. Adaptors and low-quality bases within the reads were removed using FASTX-Toolkit. The quality-filtered reads were then aligned to the *A. thaliana* genome (TAIR10) by

TopHat2, allowing no more than four mismatches (Kim et al., 2013). Uniquely aligned reads were used for calculation of FPKM. The ASEs and CPR5-regulated RASEs between WT and *cpr5* samples were defined and quantified using the ABLas pipeline (Xia et al., 2017). Briefly, ABLas pipeline detects 10 types of ASEs based on the splice junction reads, including exon skipping (ES), alternative 5′-splice site (A5SS), A3SS, IR, mutually exclusive exons (MXEs), mutually exclusive 5′-UTRs (5pMXEs), mutually exclusive 3′-UTRs (3pMXEs), cassette exon (CE), A3SS&ES, and A5SS&ES. After obtaining the ASEs in WT (as a control) and *cpr5* samples, we used Student's t test to evaluate the statistical significance of the ratio alteration of ASEs. Those ASEs at $P < 0.05$ were considered as CPR5-regulated ASEs (RASEs).

PAS-seq analysis
PAS-seq analysis was conducted at the Wuhan Ruixing Biotechnology Co., Ltd (Wuhan, China). Total RNA was treated with RQ1 DNase (Promega). The PAS-seq libraries were constructed using the SMART RT system. Briefly, polyadenylated mRNAs were purified with oligo (dT)-conjugated magnetic beads (Invitrogen) and fragmented. Reverse transcription was performed with a modified RT primer harboring dT18 and two additional anchor nucleotides at the 3′-terminus. The libraries were constructed using a ScriptSeq v2 RNA-Seq Library Preparation Kit (Illumina) and applied to Illumina HiSeq X Ten system for 150-nt paired-end sequencing. Raw reads with >3-N bases were discarded. Adaptors and low-quality bases were trimmed using FASTX-Toolkit (version 0.0.13). The short reads less than 16-nt were also dropped. The cleaned reads were searched for at least 8 consecutive poly(A) sites from the end of reads and were matched to the reference genome using TopHat2 allowing two mismatches (Kim et al., 2013). After mapping, poly(A) site information was extracted. In PAS-seq data analysis, the localization of the 3′-end of effective poly(A) reads that could be compared to the reference genome was defined as poly(A) site. To identify genes with shifted PACs, the difference of PAC locations was calculated by CAGEr to obtain shift score (Haberle et al., 2015). The Kolmogorov–Smirnov test was performed to identify significant shifts of PACs at $P < 0.01$.

GO analysis
The GO analysis was performed using GO enrichment of OmicShare (https://www.omicshare.com/tools/Home/Soft/gogseasenior).

REMSA
REMSA was carried out for evaluating RNA–protein interaction. Briefly, GST-tagged proteins were expressed in *E. coli* strain Rosetta-gami 2 (DE3; Novagen, Madison, WI, USA) and purified using BeyoGold GST-tag Purification Resin (Beyotime). RNA probes (human Tra2-targeted RNA sequence R22, AAAGAACAAGAAGAAGAAG, 20-nt) were labeled with Cy5 at the 5′-end (Sangon, Shanghai, China). RNA-protein binding buffer consists of 40-mM Tris (pH 8.0),

30-mM KCl, 1-mM MgCl$_2$, 0.01% (v/v) NP40, 1-mM DTT, 10-µg/mL bovine serum albumin (BSA), and 16 U RNase inhibitor (Beyotime). Proteins (2.5 µg) were mixed with binding buffer and incubated at room temperature for 10 min. RNA probes were heated to 94°C for 2 min followed by incubation on ice for 4 min. The denatured Cy5-labeled probes (to the final concentration of 5 nM) and non-labeled probes (in an increasing concentration gradient: 0, 1×, 5×, and 10× Cy5-labeled probes) were added to the binding reaction and incubated at 25°C for 15 min. A 5% native polyacrylamide gel in 0.5× TBE (45-mM Tris, 45-mM boric acid, 1-mM EDTA, pH 8.3) was pre-electrophoresed for 30 min. The binding reaction (15 µL) was loaded onto the pre-run gel and run at 4°C. The gels were imaged with an Azure c600 Gel Imaging System (Azure Biosystems, Dublin, CA, USA).

RIP

RIP was conducted as described (Mermaz et al., 2018). The Myc-tagged proteins were used for RIP. The RIP samples were processed without cross-linking. Anti-Myc Magnetic Beads (Bimake, Shanghai, China) were used. *ACT2* served as a negative control.

Statistics

Unless otherwise stated, statistical analysis was performed by one-way analysis of variance with Bonferroni post-hoc test. The letter above the bar indicates a statistically significant difference between groups at $P < 0.01$.

Accession numbers

All RNA-seq data have been deposited in the NCBI Sequence Read Archive (SRA) database.

RNA-seq data of WT, *cpr5*, *prl1 fip1* and *cpr5 prl1 fip1* plants for DEGs are available in the SRA database under the Bioproject accession number PRJNA737003.

RNA-seq data of WT and *cpr5* plants for RNA ASEs are available in the SRA database under the Bioproject accession number PRJNA737012.

PAS-seq data of WT and *cpr5* plants for RNA APAEs are available in the SRA database under the Bioproject accession number PRJNA737284.

The sequence of *pCas9-T1* for CRISPR/Cas9 editing is available in the GenBank database under the accession number MZ476947.

Supplemental data

The following materials are available in the online version of this article.

Supplemental Figure S1. Cloning and epistatic analysis of the *SCPR* genes.

Supplemental Figure S2. Genome-wide profiling of the PRL1/FIP1-dependent genes in *cpr5* mutant.

Supplemental Figure S3. Alignment of CPR5 proteins and Tra2 subfamily proteins.

Supplemental Figure S4. CPR5 interacts with PRL1 and FIP1.

Supplemental Figure S5. The CPR5-regulated splicing and polyadenylation.

Supplemental Table S1. Single SNPs in *scpr44* and *scpr57* mutants.

Supplemental Table S2. Primers used in this study.

Supplemental File S1. The sequences of the Tra2 subfamily proteins used for the phylogenetic analysis.

Supplemental Data Set 1. DEGs between WT, *cpr5*, *prl1 fip1*, and *cpr5 prl1 fip1* plants.

Supplemental Data Set 2. DEGs, ASGs, and APAGs between WT and *cpr5* plants.

Reference

Bao Z, Yang H, Hua J (2013) Perturbation of cell cycle regulation triggers plant immune response via activation of disease resistance genes. Proc Natl Acad Sci USA **110**: 2407–2412

Baulcombe D (2004) RNA silencing in plants. Nature **431**: 356–363

Bazin J, Mariappan K, Jiang Y, Blein T, Voelz R, Crespi M, Hirt H (2020) Role of MPK4 in pathogen-associated molecular pattern-triggered alternative splicing in Arabidopsis. PLoS Pathog **16**: e1008401

Bhattacharjee S, Halane MK, Kim SH, Gassmann W (2011) Pathogen effectors target Arabidopsis EDS1 and alter its interactions with immune regulators. Science **334**: 1405–1408

Bohm H, Albert I, Fan L, Reinhard A, Nurnberger T (2014) Immune receptor complexes at the plant cell surface. Curr Opin Plant Biol **20**: 47–54

Bowling SA, Clarke JD, Liu Y, Klessig DF, Dong X (1997) The cpr5 mutant of Arabidopsis expresses both NPR1-dependent and NPR1-independent resistance. Plant Cell **9**: 1573–1584

Bruggeman Q, Garmier M, de Bont L, Soubigou-Taconnat L, Mazubert C, Benhamed M, Raynaud C, Bergounioux C, Delarue M (2014) The polyadenylation factor subunit CLEAVAGE AND POLYADENYLATION SPECIFICITY FACTOR30: a key factor of programmed cell death and a regulator of immunity in Arabidopsis. Plant Physiol **165**: 732–746

Calabretta, S, Richard, S (2015) Emerging roles of disordered sequences in RNA-binding proteins. Trends Biochem Sci **40**: 662–672

Califice S, Baurain D, Hanikenne M, Motte P (2012) A single ancient origin for prototypical serine/arginine-rich splicing factors. Plant Physiol **158**: 546–560

Cao H, Glazebrook J, Clarke JD, Volko S, Dong X (1997) The Arabidopsis NPR1 gene that controls systemic acquired resistance encodes a novel protein containing ankyrin repeats. Cell **88**: 57–63

Chan SP, Kao DI, Tsai WY, Cheng SC (2003) The Prp19p-associated complex in spliceosome activation. Science **302**: 279–282

Cheng YT, Germain H, Wiermer M, Bi D, Xu F, Garcia AV, Wirthmueller L, Despres C, Parker JE, Zhang Y, et al. (2009) Nuclear pore complex component MOS7/Nup88 is required for innate immunity and nuclear accumulation of defense regulators in Arabidopsis. Plant Cell 21: 2503–2516

Deka B, Singh KK (2017) Multifaceted regulation of gene expression by the apoptosis- and splicing-associated protein complex and its components. Int J Biol Sci 13: 545–560

Dereeper A, Guignon V, Blanc G, Audic S, Buffet S, Chevenet F, Dufayard JF, Guindon S, Lefort V, Lescot M, et al. (2008) Phylogeny.fr: robust phylogenetic analysis for the non-specialist. Nucleic Acids Res 36: W465–W469

Dinesh-Kumar SP, Baker BJ (2000) Alternatively spliced N resistance gene transcripts: Their possible role in tobacco mosaic virus resistance. Proc Natl Acad Sci U S A 97: 1908–1913

Elkon R, Ugalde AP, Agami R (2013) Alternative cleavage and polyadenylation: extent, regulation and function. Nat Rev Genet 14: 496–506

Fassler F, Pimpl P (2017) In Vivo interaction studies by measuring Forster resonance energy transfer through fluorescence lifetime imaging microscopy (FRET/FLIM). Methods Mol Biol 1662: 159–170

Fu ZQ, Guo M, Jeong BR, Tian F, Elthon TE, Cerny RL, Staiger D, Alfano JR (2007) A type III effector ADP-ribosylates RNA-binding proteins and quells plant immunity. Nature 447: 284–288

Graub R, Lancero H, Pedersen A, Chu M, Padmanabhan K, Xu XQ, Spitz P, Chalkley R, Burlingame AL, Stokoe D, et al. (2008) Cell cycle-dependent phosphorylation of human CDC5 regulates RNA processing. Cell Cycle 7: 1795–1803

Gu Y, Zebell SG, Liang Z, Wang S, Kang BH, Dong X (2016) Nuclear pore permeabilization is a convergent signaling event in effector-triggered immunity. Cell 166: 1526–1538

Haberle V, Forrest AR, Hayashizaki Y, Carninci P, Lenhard B (2015) CAGEr: precise TSS data retrieval and high-resolution promoterome mining for integrative analyses. Nucleic Acids Res 43: e51.

Heidrich K, Wirthmueller L, Tasset C, Pouzet C, Deslandes L, Parker JE (2011) Arabidopsis EDS1 connects pathogen effector recognition to cell compartment-specific immune responses. Science 334: 1401–1404

Hoshijima K, Inoue K, Higuchi I, Sakamoto H, Shimura Y (1991) Control of doublesex alternative splicing by transformer and transformer-2 in Drosophila. Science 252: 833–836

Huang S, Zhu S, Kumar P, MacMicking JD (2021) A phase-separated nuclear GBPL circuit controls immunity in plants. Nature 594: 424–429

Jia T, Zhang B, You C, Zhang Y, Zeng L, Li S, Johnson K, Yu B, Li X, Chen X (2017) The Arabidopsis MOS4-associated complex promotes microRNA biogenesis and precursor messenger RNA splicing. Plant Cell 29: 2626–2643

Jing HC, Anderson L, Sturre MJ, Hille J, Dijkwel PP (2007) Arabidopsis CPR5 is a senescence-regulatory gene with pleiotropic functions as predicted by the evolutionary theory of senescence. J Exp Bot 58: 3885–3894

Johnson KC, Dong OX, Huang Y, Li X (2012) A rolling stone gathers no moss, but resistant plants must gather their moses. Cold Spring Harb Symp Quant Biol 77: 259–268

Jones JD, Dangl JL (2006) The plant immune system. Nature 444: 323–329

Kalyna M, Barta A (2004) A plethora of plant serine/arginine-rich proteins: redundancy or evolution of novel gene functions? Biochem Soc Trans 32: 561–564

Kim D, Pertea G, Trapnell C, Pimentel H, Kelley R, Salzberg SL (2013) TopHat2: accurate alignment of transcriptomes in the presence of insertions, deletions and gene fusions. Genome Biol 14: R36

Kunkel BN, Bent AF, Dahlbeck D, Innes RW, Staskawicz BJ (1993) RPS2, an Arabidopsis disease resistance locus specifying recognition of Pseudomonas syringae strains expressing the avirulence gene avrRpt2. Plant Cell 5: 865–875

Lamond AI, Spector DL (2003) Nuclear speckles: a model for nuclear organelles. Nat Rev Mol Cell Biol 4: 605–612

Lareau LF, Inada M, Green RE, Wengrod JC, Brenner SE (2007) Unproductive splicing of SR genes associated with highly conserved and ultraconserved DNA elements. Nature 446: 926–929

Li X, Kapos P, Zhang Y (2015) NLRs in plants. Curr Opin Immunol 32: 114–121

Li Y, Zhang Q, Zhang J, Wu L, Qi Y, Zhou JM (2010) Identification of microRNAs involved in pathogen-associated molecular pattern-triggered plant innate immunity. Plant Physiol 152: 2222–2231

Li Y, Guo Q, Liu P, Huang J, Zhang S, Yang G, Wu C, Zheng C, Yan K (2021) Dual roles of the serine/arginine-rich splicing factor SR45a in promoting and interacting with nuclear cap-binding complex to modulate the salt-stress response in Arabidopsis. New Phytol 230: 641–655

Loyer P, Trembley JH (2020) Roles of CDK/Cyclin complexes in transcription and pre-mRNA splicing: cyclins L and CDK11 at the cross-roads of cell cycle and regulation of gene expression. Semin Cell Dev Biol 107: 36–45

Mermaz B, Liu F, Song J (2018) RNA immunoprecipitation protocol to identify protein-RNA interactions in Arabidopsis thaliana. Methods Mol Biol 1675: 331–343

Misra A, Green MR (2016) From polyadenylation to splicing: dual role for mRNA 3' end formation factors. Rna Biol 13: 259–264

Misra A, Ou J, Zhu LJ, Green MR (2015) Global promotion of alternative internal exon usage by mRNA 3' end formation factors. Mol Cell 58: 819–831

Monaghan J, Xu F, Gao M, Zhao Q, Palma K, Long C, Chen S, Zhang Y, Li X (2009) Two Prp19-like U-box proteins in the MOS4-associated complex play redundant roles in plant innate immunity. PLoS Pathog 5: e1000526

Moore JW, Loake GJ, Spoel SH (2011) Transcription dynamics in plant immunity. Plant Cell 23: 2809–2820

Nemeth K, Salchert K, Putnoky P, Bhalerao R, Koncz-Kalman Z, Stankovic-Stangeland B, Bako L, Mathur J, Okresz L, Stabel S, et al. (1998) Pleiotropic control of glucose and hormone responses by PRL1, a nuclear WD protein, in Arabidopsis. Genes Dev 12: 3059–3073

Nicaise V, Joe A, Jeong BR, Korneli C, Boutrot F, Westedt I, Staiger D, Alfano JR, Zipfel C (2013) Pseudomonas HopU1 modulates plant immune receptor levels by blocking the interaction of their mRNAs with GRP7. EMBO J 32: 701–712

Palma K, Zhao Q, Cheng YT, Bi D, Monaghan J, Cheng W, Zhang Y, Li X (2007) Regulation of plant innate immunity by three proteins in a complex conserved across the plant and animal kingdoms. Genes Dev 21: 1484–1493

Pan Q, Shai O, Lee LJ, Frey BJ, Blencowe BJ (2008) Deep surveying of alternative splicing complexity in the human transcriptome by high-throughput sequencing. Nat Genet 40: 1413–1415

Peng S, Sun K, Guo Y, Liu Y, Wang S (2020) Arabidopsis nucleoporin CPR5 controls trichome cell death through the core cell cycle regulator CKI. Plant Biol (Stuttg) 22: 337–345

Preker PJ, Lingner J, Minvielle-Sebastia L, Keller W (1995) The FIP1 gene encodes a component of a yeast pre-mRNA polyadenylation factor that directly interacts with poly(A) polymerase. Cell 81: 379–389

Ramirez-Prado JS, Abulfaraj AA, Rayapuram N, Benhamed M, Hirt H (2018) Plant immunity: from signaling to epigenetic control of defense. Trends Plant Sci 23: 833–844

Reichholf B, Herzog VA, Fasching N, Manzenreither RA, Sowemimo I, Ameres SL (2019) Time-resolved small RNA sequencing unravels the molecular principles of microRNA homeostasis. Mol Cell 75: 756–768

Shen QH, Schulze-Lefert P (2007) Rumble in the nuclear jungle: compartmentalization, trafficking, and nuclear action of plant immune receptors. EMBO J 26: 4293–4301

Sherstnev A, Duc C, Cole C, Zacharaki V, Hornyik C, Ozsolak F, Milos PM, Barton GJ, Simpson GG (2012) Direct sequencing of *Arabidopsis thaliana* RNA reveals patterns of cleavage and polyadenylation. Nat Struct Mol Biol **19**: 845–852

Snead WT, Gladfelter AS (2019) The control centers of biomolecular phase separation: how membrane surfaces, PTMs, and active processes regulate condensation. Mol Cell **76**: 295–305

Staiger D, Korneli C, Lummer M, Navarro L (2013) Emerging role for RNA-based regulation in plant immunity. New Phytol **197**: 394–404

Stemmer M, Thumberger T, Del SKM, Wittbrodt J, Mateo JL (2015) CCTop: an intuitive, flexible and reliable CRISPR/Cas9 target prediction tool. PLoS One **10**: e124633

Tacke R, Tohyama M, Ogawa S, Manley JL (1998) Human Tra2 proteins are sequence-specific activators of pre-mRNA splicing. Cell **93**: 139–148

Tian B, Manley JL (2017) Alternative polyadenylation of mRNA precursors. Nat Rev Mol Cell Biol **18**: 18–30

Valcarcel J, Green MR (1996) The SR protein family: pleiotropic functions in pre-mRNA splicing. Trends Biochem Sci **21**: 296–301

Vi SL, Trost G, Lange P, Czesnick H, Rao N, Lieber D, Laux T, Gray WM, Manley JL, Groth D, et al. (2013) Target specificity among canonical nuclear poly(A) polymerases in plants modulates organ growth and pathogen response. Proc Natl Acad Sci USA **110**: 13994–13999

Wan R, Bai R, Zhan X, Shi Y (2020) How is precursor messenger RNA spliced by the spliceosome? Annu Rev Biochem **89**: 333–358

Wang S (2017) The CPR5-CKI signaling pathway plays a central role in integrating plant stress responses. Can J Plant Sci **97**: 767–770

Wang S, Gu Y, Zebell SG, Anderson LK, Wang W, Mohan R, Dong X (2014) A noncanonical role for the CKI-RB-E2F cell-cycle signaling pathway in plant effector-triggered immunity. Cell Host Microbe **16**: 787–794

Wildermuth MC, Steinwand MA, McRae AG, Jaenisch J, Chandran D (2017) Adapted biotroph manipulation of plant cell ploidy. Annu Rev Phytopathol **55**: 537–564

Wilson IA, Haft DH, Getzoff ED, Tainer JA, Lerner RA, Brenner S (1985) Identical short peptide sequences in unrelated proteins can have different conformations: a testing ground for theories of immune recognition. Proc Natl Acad Sci USA **82**: 5255–5259

Wootton JC (1994) Non-globular domains in protein sequences: automated segmentation using complexity measures. Comput Chem **18**: 269–285

Xia H, Chen D, Wu Q, Wu G, Zhou Y, Zhang Y, Zhang L (2017) CELF1 preferentially binds to exon-intron boundary and regulates alternative splicing in HeLa cells. Biochim Biophys Acta Gene Regul Mech **1860**: 911–921

Xu F, Jia M, Li X, Tang Y, Jiang K, Bao J, Gu Y (2021) Exportin-4 coordinates nuclear shuttling of TOPLESS family transcription corepressors to regulate plant immunity. Plant Cell **33**: 697–713

Xu F, Xu S, Wiermer M, Zhang Y, Li X (2012) The cyclin L homolog MOS12 and the MOS4-associated complex are required for the proper splicing of plant resistance genes. Plant J **70**: 916–928

Xu S, Zhang Z, Jing B, Gannon P, Ding J, Xu F, Li X, Zhang Y (2011) Transportin-SR is required for proper splicing of resistance genes and plant immunity. PLoS Genet **7**: e1002159.

Zhang XC, Gassmann W (2003) RPS4-Mediated Disease Resistance Requires the Combined Presence of RPS4 Transcripts with Full-Length and Truncated Open Reading Frames. Plant Cell **15**: 2333–2342

Zhang N, Wang Z, Bao Z, Yang L, Wu D, Shu X, Hua J (2018) MOS1 functions closely with TCP transcription factors to modulate immunity and cell cycle in Arabidopsis. Plant J **93**: 66–78

Zhang R, Calixto C, Marquez Y, Venhuizen P, Tzioutziou NA, Guo W, Spensley M, Entizne JC, Lewandowska D, Ten HS, Frei DFN, Hirt H, James AB, Nimmo HG, Barta A, Kalyna M, and Brown J et al. (2017a) A high quality Arabidopsis transcriptome for accurate transcript-level analysis of alternative splicing. Nucleic Acids Res **45**: 5061-–5073.

Zhang Y, Goritschnig S, Dong X, and Li X (2003) A gain-of-function mutation in a plant disease resistance gene leads to constitutive activation of downstream signal transduction pathways in suppressor of npr1-1, constitutive 1. Plant Cell **15**: 2636-–2646.

Zhang Y, Li X (2005) A putative nucleoporin 96 Is required for both basal defense and constitutive resistance responses mediated by suppressor of npr1-1, constitutive 1. Plant Cell **17**: 1306–1316.

Zhang XN, Shi Y, Powers JJ, Gowda NB, Zhang C, Ibrahim H, Ball HB, Chen SL, Lu H, and Mount SM (2017b) Transcriptome analyses reveal SR45 to be a neutral splicing regulator and a suppressor of innate immunity in *Arabidopsis thaliana*. BMC Genomics **18**: 772.